Self-organized criticality

Donald L Turcotte

Department of Geological Sciences, Cornell University, Snee Hall, Ithaca, NY 14853-1504, USA

Abstract

The concept of self-organized criticality was introduced to explain the behaviour of the sandpile model. In this model, particles are randomly dropped onto a square grid of boxes. When a box accumulates four particles they are redistributed to the four adjacent boxes or lost off the edge of the grid. Redistributions can lead to further instabilities with the possibility of more particles being lost from the grid, contributing to the size of each 'avalanche'. These model 'avalanches' satisfied a power-law frequency–area distribution with a slope near unity. Other cellular-automata models, including the slider-block and forest-fire models, are also said to exhibit self-organized critical behaviour. It has been argued that earthquakes, landslides, forest fires, and species extinctions are examples of self-organized criticality in nature. In addition, wars and stock market crashes have been associated with this behaviour. The forest-fire model is particularly interesting in terms of its relation to the critical-point behaviour of the site-percolation model. In the basic forest-fire model, trees are randomly planted on a grid of points. Periodically in time, sparks are randomly dropped on the grid. If a spark drops on a tree, that tree and adjacent trees burn in a model fire. The fires are the 'avalanches' and they are found to satisfy power-law frequency–area distributions with slopes near unity. This forest-fire model is closely related to the site-percolation model, that exhibits critical behaviour. In the forest-fire model there is an inverse cascade of trees from small clusters to large clusters, trees are lost primarily from model fires that destroy the largest clusters. This quasi steady-state cascade gives a power-law frequency–area distribution for both clusters of trees and smaller fires. The site-percolation model is equivalent to the forest-fire model without fires. In this case there is a transient cascade of trees from small to large clusters and a power-law distribution is found only at a critical density of trees.

Contents

1. Introduction

The concept of self-organized criticality was proposed by Bak *et al* (1987, 1988) as an explanation for the behaviour of a cellular-automata model they developed. In this model there is a square grid of boxes and at each time step a particle is dropped into a randomly selected box. When a box accumulates four particles, the particles are redistributed to the four neighbouring boxes, or in the case of edge boxes, lost from the grid. Redistributions can lead to further instabilities, with 'avalanches' of particles lost from the edge of the grid. Because of this 'avalanche' behaviour, this was called a 'sandpile' model. The noncumulative frequency–area distribution of model 'avalanches' was found to satisfy a power-law (fractal) distribution

$$N \sim A^{-\alpha} \tag{1.1}$$

where N is the number of avalanches with area A and α is a constant with a value $\alpha \approx 1$.

A second model that can exhibit self-organized critical behaviour is the slider-block model (Carlson and Langer 1989a, b). In this model, an array of slider blocks are connected to a constant velocity driver plate by puller springs and to each other by connector springs. The blocks exhibit stick–slip behaviour due to frictional interactions with the plate across which they are pulled. The frequency–area distribution of the smaller slip events again satisfies (1.1) with $\alpha \approx 1$. The area A is defined to be the number of blocks that participate in a slip event. This model is completely deterministic whereas the sandpile model is stochastic. This model also provides a direct bridge to deterministic chaos; for instance, Huang and Turcotte (1990a) showed that a pair of slider blocks pulled over a surface can exhibit deterministic chaos with a period doubling route to chaos.

A third model that exhibits deterministic chaos is the forest-fire model (Bak *et al* 1992, Drossel and Schwabl 1992a, b). In the simplest version of this model, a square grid of sites is considered. At each time step either a tree is planted on a randomly chosen site (if the site is unoccupied) or a spark is dropped on the site. If the spark is dropped on a tree, that tree and all adjacent trees are 'burned' in a model 'forest fire'. The frequency–area distribution of the smaller fires again satisfies (1.1) with $\alpha = 1.0–1.2$. The area A is defined to be the number of trees that are burned in a fire. The forest-fire model is closely related to the site-percolation model that is known to exhibit critical behaviour (Stauffer and Aharony 1992). If trees are planted on a grid without fires, site-percolation behaviour is found. The critical point is reached when a tree cluster spans the grid.

A satisfactory definition for self-organized criticality remains elusive. The three models discussed above exhibit similar behaviours but there are also significant differences. Many variations on these models have been proposed; some are considered self-organized critical but many others are not. Totally different models have been proposed that exhibit self-organized critical behaviour. Some of these models are applicable to problems in the biological and social sciences. Bak (1996) has provided a comprehensive, if personal, review of developments. An extensive discussion of self-organized criticality has also been given by Jensen (1998).

Shortly after the 'sandpile' model was proposed a number of laboratory studies were undertaken to determine whether actual sandpiles exhibit the behaviour attributed to self-organized criticality. A variety of frequency–size statistics for avalanches were found (Nagel 1992, Feder 1995); in some cases the results were consistent with the power-law relation (1.1), but in other cases they were not.

Although the concept of self-organized criticality was conceived as an explanation for simple 'toy' models, it has been associated with several natural hazards (Malamud and Turcotte 1999). Examples include the following:

(1) *Earthquakes*. Stress accumulates on time scales of hundreds to thousands of years due to the slow movement of the tectonic plates. Stress is relieved in seconds during earthquakes. Earthquakes in a region occur on a mosaic of faults. A universal feature of earthquakes in a region is that they satisfy the power-law relation (1.1) with a near universal value of α. However, for earthquakes, $\alpha \approx 2$ rather than the $\alpha \approx 1$ associated with the models discussed above.

(2) *Forest and wild fires*. Combustible material grows on long time scales and is destroyed in fires on short time scales. The frequency–area distribution of forest and wild fires is well approximated by the power-law relation (1.1) with $\alpha = 1.3$–1.5.

(3) *Landslides*. Slope instabilities develop slowly and are relieved on short time scales in landslides. The frequency–area distribution of landslides is well approximated by the power-law relation (1.1) with $\alpha = 2.3$–3.3.

Applications of self-organized criticality have also been proposed in the biological and social sciences. Some examples are the following:

(1) *Biodiversity*. The diversity of species develops on long time scales and is wiped out in extinctions on short time scales. There is some indication that the frequency–size distribution of extinction events is power-law.

(2) *Epidemics*. A population develops that has little immunity to diseases over long time scales. The disease spreads as an epidemic on a short time scale. Again there is some evidence that the frequency–size distribution of epidemics is power-law.

(3) *Wars*. Instabilities between countries develop on relatively long time scales terminating in wars that generally last relatively short periods of time. Richardson (1941) measured the intensity of wars in terms of the numbers of battle deaths and showed that the frequency–intensity distribution of wars is well approximated by a power-law distribution.

(4) *Stock-market crashes*. Stock markets expand and grow on relatively long time scales but contract in stock-market crashes on relatively short time scales.

A rigorous definition of self-organized critical behaviour is elusive. A working definition is that a system is in a state of self-organized criticality if a measure of the system fluctuates about a state of marginal stability. In self-organized criticality, the 'input' to a complex system is constant, whereas the 'output' is a series of events or 'avalanches' that follow a power-law (fractal) frequency–size distribution. For example, in the case of the sandpile model, the input is the steady addition of sand grains, and the output is sand avalanches.

Power-law (fractal) frequency–size distributions can be explained in terms of scale invariance. The power-law distribution is the only distribution that does not require a characteristic length scale. Thus, natural phenomena that do not inherently have a natural length scale (i.e. that are scale invariant) would be expected to follow a power-law (fractal) distribution. In the past ten years, numerous numerical models have been found that are believed to exhibit self-organized critical behaviour; many believe this universal behaviour is a fundamental basis for the applicability of fractal statistics.

In this review we begin by discussing the sandpile, slider-block and forest-fire models in detail and the relation these models have with the idea of self-organized criticality. In addition to an overall view of the mathematical formalism and statistics of each cellular-automata model, and how each model relates to the other, we will discuss and provide a review of the many 'applications' of these models in both the laboratory and the real world. We follow these sections with one that discusses the inverse-cascade and site-percolation models and a comparison of self-organized criticality and criticality. The final sections in this review provide a detailed review of self-organized criticality applied to the physical, biological and social sciences.

2. Sandpile model

2.1. Cellular-automata model

The concept of self-organized criticality evolved from the 'sandpile' model proposed by Bak *et al* (1987, 1988). In this model there is a square grid of boxes and at each time step a particle is dropped into a randomly selected box. When a box accumulates four particles, they are redistributed to the four adjacent boxes, or in the case of edge boxes they are lost from the grid. Since only nearest-neighbour boxes are involved in a redistribution, this is a cellular-automata model. Redistributions can lead to further instabilities and avalanches of particles in which many particles may be lost from the edges of the grid. The input is the steady-state addition of particles. A measure of the state of the system is the average number of particles in the boxes. This 'density' fluctuates about a quasi-equilibrium value. Each of the multiple redistributions during a time step contributes to the size of the model 'avalanche'. One measure of the size of a model avalanche is given by the number of particles lost from the grid during each sequence of redistributions; an alternative measure is given by the number of boxes that participate in the redistributions.

This model was called a 'sandpile' model because of the resemblance to an actual sandpile on a table. The randomly dropped particles in the model are analogous to the addition of particles to an actual sandpile and the model avalanches are analogous to sand avalanches down the sides of the sandpile. In some cases the sand avalanches lead to the loss of particles off the table.

The sandpile model depends only on the size of the grid considered. As a specific example of the sandpile model, consider the 3×3 grid illustrated in figure 1. As shown, each box is identified by a row and column. The simulation has been run for some time so that a quasi-equilibrium beginning configuration has been established. In steps 1–4, particles have been added randomly to cells '22', '00', '11' and '12' without requiring any redistributions. In step 5a, a particle is added to box '11'; this box is now 'unstable' and the four particles are redistributed to the adjacent boxes '01', '10', '12' and '21'. This redistribution causes three of these boxes, '01', '10', '12' and '21' to become unstable, requiring further redistributions. The selection of which box to redistribute next is arbitrary; however, the choice does not influence the statistical evolution of the model. In step 5c, the four particles in box '01' are redistributed: one particle is lost from the grid and particles are added to boxes '00', '02', and '11'. Eight further redistributions are required before an 'equilibrium' configuration (all boxes with less than four particles) is reached. These redistributions are illustrated in steps 5d–5k. During this sequence of redistributions, all nine boxes were unstable and box '11' was unstable twice. During the sequence of redistributions, 12 particles were lost from the grid and the number of particles on the grid was reduced from 25 to 13. In step 6a, a particle is added to box '01' and it is unstable. A single redistribution is required and one particle is lost from the grid.

Having specified the size of the grid, a simulation is run for N_S time steps and the number of avalanches N_L with area A_L is determined. The area A_L is defined to be the number of boxes that participate in an avalanche. The noncumulative frequency–area distribution for model avalanches is given for a 50×50 grid in figure 2. There is a good correlation with the power-law relation (1.1) with $\alpha \approx 1.0$. Large-scale simulations (Kadanoff *et al* 1989, Manna 1990, Lubeck and Usadel 1997) show that this correlation is valid over the entire range of areas from a single box to the entire grid and is independent of the size of the grid.

The time series associated with the average number of particles in the boxes has been said to exhibit $1/f$ or red noise, where f is the frequency (Bak *et al* 1987, 1988). If the time T associated with an avalanche is taken to be the number of particle redistributions during an
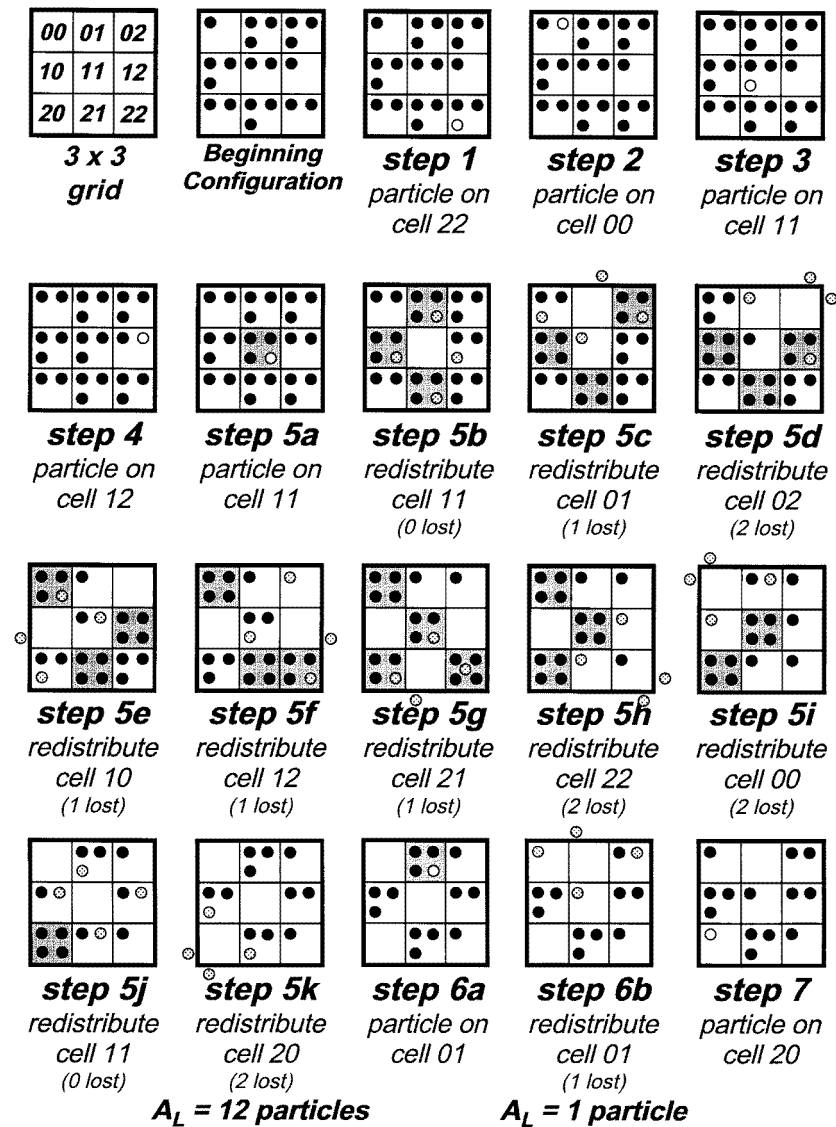
Figure 1. Illustration of the sandpile model. A 3 x 3 grid is considered and seven time steps are shown. Model 'avalanches' occur in steps 5 and 6. For the first avalanche, there are ten required redistributions (steps 5b–5k), all nine boxes were 'unstable' at least once, and 12 particles were lost from the grid. In the second avalanche, only one box became unstable, and only one particle was lost from the grid.

avalanche, it is found that

$$N \sim T^{-1} \tag{2.1}$$

where N is the number of events with T redistributions. This was the basis for the $1/f$ argument. However, the usual definition of a $1/f$ noise is in terms of the power spectral density S with

$$S \sim f^{-\beta}. \tag{2.2}$$
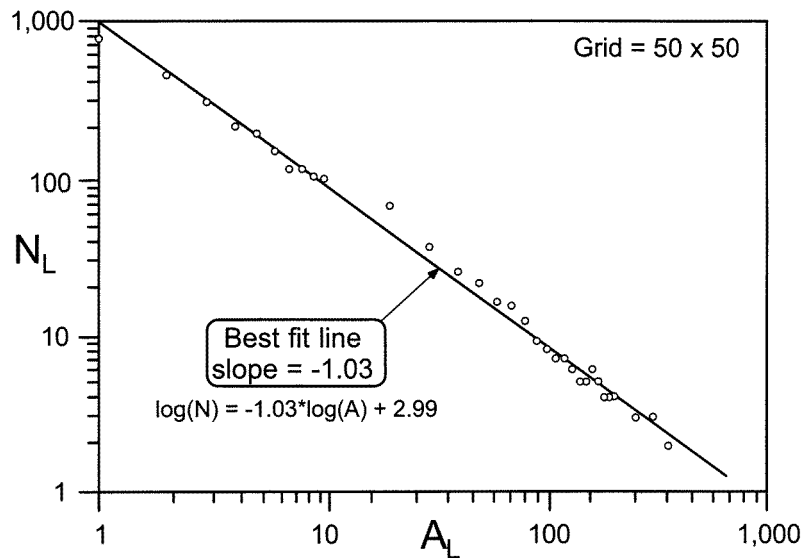
Figure 2. Noncumulative frequency–area distribution for a sandpile model on a 50×50 grid. The number of model events, N_L, in which a specified number of boxes, A_L, become unstable, is given as a function of A_L.

When the actual time series behaviour of the sandpile model is studied it is found that $\beta \approx 2$ (Jensen *et al* 1989, Kertesz and Kiss 1990, O'Brien and Weissman 1992).

Dhar (1990) has shown that the sandpile model described above is Abelian, i.e. the final state of the system is independent of the order in which steps are taken. One consequence of this is that the order in which redistributions are carried out during an avalanche does not affect the final structure of the avalanche (Dhar and Majumdar 1990, Majumdar and Dhar 1992, Speer 1993, Ivashkevich *et al* 1994, Dhar *et al* 1995, Dhar 1996, 1999, Tsuchiya and Katori 1999).

The only control parameter in this model is the size of the square grid of boxes. This size limits the size of the largest model avalanche but does not otherwise influence the behaviour of the model. The frequency–area distribution of avalanches is power-law (fractal) whether the area of the avalanche is specified by the number of particles lost from the grid or by the number of boxes that participate in the avalanche. Thus the behaviour of the system is scale invariant. It is also important to note that the slope of the power-law distribution is close to unity in many examples.

When first introduced, the 'sandpile' model created a great deal of interest because of its unusual behaviour. It is not a critical problem because there is no control parameter to tune. The behaviour of the system does not approach a well-defined equilibrium and it does not diverge to infinity. The system fluctuates about a quasi-equilibrium density of particles. Particles accumulate slowly as they are randomly added to boxes and are lost precipitously in model avalanches. Because of this great interest many variations on this basic 'sandpile' model have been studied. Some exhibit a similar type of behaviour and others do not. Variations include studies of the one-dimensional version (Ali and Dhar 1995a, b, Chang *et al* 1995, Kutnjak-Urbanc *et al* 1996a, Head and Rodgers 1997a, Pinho *et al* 1997, Priezzhev and Sneppen 1998), the three-dimensional version (Robinson 1994), singular diffusion (Carlson *et al* 1990), and a slope instability rather than a height instability (Chhabra *et al* 1993). Variations have been

studied that are directed (Dhar and Ramaswamy 1989) and dissipative (Bak 1992, Christensen *et al* 1992, Lauritsen *et al* 1996, Lise and Jensen 1996, Chabanol and Hakim 1997, Ruskin and Feng 1997, Dickman *et al* 1998). An example of a dissipative model is one where only a fraction of the particles in a box are redistributed to other boxes. Many other techniques have been applied to the analyses of sandpile models. Examples include mean-field studies (Alstrom 1988, Tang and Bak 1988a, Gaveau and Schulman 1991, Janowsky and Laberge 1993, Katori and Kobayashi 1993, Zapperi *et al* 1995, Vergeles *et al* 1997, Vespignani and Zapperi 1997, 1998), universality (Chessa *et al* 1999), renormalization group methods (Pietronero *et al* 1994, Vespignani *et al* 1995), branching processes (Ivashkevich 1996), invasion percolation (Roux and Guyon 1989) and damage analysis (Bhowal 1997). Authors have considered time-dependent toppling rules (Broker 1996), hot sandpiles (Caldarelli *et al* 1996b, Vergeles 1997) and many other topics (Tang and Bak 1988b, Wiesenfeld *et al* 1989, 1990, Zhang 1989, Bak 1990, Grassberger and Manna 1990, Grinstein *et al* 1990, Manna *et al* 1990, McNamara and Wiesenfeld 1990, Christensen *et al* 1991, Majumdar and Dhar 1991, Manna 1991a, b, Pietronero and Schneider 1991, Diaz-Guilera 1992, Tadic *et al* 1992, Christensen and Olami 1993, Socolar *et al* 1993, Bak and Creutz 1994, Bonabeau and Lederer 1994, Dhar and Manna 1994, Family 1994, Garcia-Pelayo 1994, Priezzhev 1994, Cafiero *et al* 1995, Maslov and Zhang 1995, Pietronero 1995, Stella *et al* 1995, Ben-Hur and Biham 1996, Flyvbjerg 1996, Gil and Sornette 1996, Lubeck *et al* 1996, Priezzhev *et al* 1996, Lubeck 1997, Manna and Giri 1997, Tadic and Dhar 1997, Ceva and Luzuriaga 1998, Chessa *et al* 1998, Ivashkevich and Priezzhev 1998, Milshtein *et al* 1998, Kinouchi and Prado 1999, Tsuchiya and Katori 1999).

Barriere and Turcotte (1991, 1994), Kutnjak-Urbanc *et al* (1996b), and Daerden and Vanderzande (1998) studied 'sandpile' models with a power-law distribution of box sizes. Redistributions from a large box always generated instabilities in adjacent smaller boxes. These are very similar to the aftershock sequence following earthquakes. In some cases a redistribution from a smaller box generated an instability in a larger box. This is analogous to the occurrence of a foreshock before an earthquake. Edney *et al* (1998) have determined and compared the critical exponents for eight sandpile models.

2.2. Laboratory sandpiles

A direct analogy can be made between the sandpile model and avalanches on actual sandpiles. Consider a pile of sand on a circular table. Grains of sand are randomly dropped on the pile until the slope of the pile reaches the critical angle of internal friction. This is the maximum slope that a granular material can maintain without additional grains sliding down the slope; in the case of sands, these angles are typically 34–37°. One hypothesis for the behaviour of the sandpile would be that individual grains could be added until the slope is everywhere at an angle of repose. Additional grains would then simply slide down the slope. This is not what happens. The sandpile never reaches the hypothetical critical state. As the critical state is approached, additional sand grains trigger avalanches of various sizes. On average, the number of sand grains added balance the number that slide down the slope and off the table.

In order to test the applicability of the 'sandpile' model, many laboratory studies have been carried out on actual sandpiles. The approach just discussed drops individual sand grains onto a table until sand avalanches occur on the resulting sandpile. However, a preferred configuration was to study a rotating drum half-filled with sand. From the classical point of view, the flat surface will be rotated until the static angle of repose is reached. At this time an avalanche is initiated and the avalanche will continue until the dynamic angle of repose is reached. Periodic large avalanches would be expected. However, if the results of the 'sandpile' model are applicable, a power-law distribution of avalanche sizes would be expected. Laboratory

experiments have been carried out using spherical glass beads, rough aluminium particles, rice grains and other granular materials in addition to sand. Frequency–volume distributions for avalanches were obtained.

Experimental results have been quite ambiguous. Certainly not all studies exhibited power-law distributions of avalanches. In some cases the results were dominated by quasi-periodic large avalanches (Evesque and Rajchenbach 1989, Jaeger *et al* 1989, Evesque 1991a, b, Evesque *et al* 1993) and in other cases a power-law distribution was a good approximation for the observed results (Rosendahl *et al* 1993, 1994, Somfai *et al* 1994, Frette *et al* 1996). Bretz *et al* (1992) observed periodic large avalanches and a near-power-law distribution of small avalanches. Held *et al* (1990) found power-law distributions for small sandpiles but not for large sandpiles. A variety of other studies have been carried out (Puhl 1992, Frette 1993, Grumbacher *et al* 1993, Baumann and Wolf 1996, Christensen *et al* 1996, Densmore *et al* 1997, Hager *et al* 1997, Head and Rodgers 1997b, 1999). Laboratory studies of sandpiles have been reviewed by Nagel (1992) and Feder (1995).

Numerical studies of sandpile avalanches have also carried out with mixed results (Mehta and Barker 1994a, b, Buchholtz and Poschel 1996, Malthe-Sorenssen 1996, Boguna and Corral 1997, Zhang 1997, Manna and Khakhar 1998). Dhar (1992) and Prado and Olami (1992) have suggested that the reason that laboratory experiments do not generate power-law avalanche distributions is due to inertial effects. This explanation is consistent with the experimental studies of avalanches on rice piles carried out by Frette *et al* (1996). They found power-law distributions for elongated grains in which inertial effects were minimized and deviations for more circular rice grains.

When droplets of water fall on an inclined glass plate they adhere to the plate due to surface tension. If there are enough water droplets, however, rivelets of water cascade down the plate. These rivelets can be considered to be 'avalanches' in the sense of the sandpile model. Plourde *et al* (1993) carried out laboratory studies of this problem and found that the frequency–size distribution of rivelets was a power law.

2.3. Landslides

We now turn our attention to the frequency–area distributions of actual landslides. A number of studies (Whitehouse and Griffiths 1983; Ohmori and Hirano 1988, Sasaki *et al* 1991, Noever 1993, Sugai *et al* 1994, Yokoi *et al* 1995, Hovius *et al* 1997) have presented evidence that landslide frequency–area distributions are often well represented by the power-law relation (1.1).

When considering actual data, results are generally presented using cumulative statistics; for instance, the cumulative number of landslides N_{CL} with areas greater than A_L are plotted as a function of A_L. However, the frequency–area distribution for the model avalanches given in figure 2 is noncumulative, i.e. the data is given in terms of unit steps of area. In order to make a direct comparison of the sandpile model results with actual landslides, the noncumulative model data could be converted to a cumulative distribution by summing model avalanches larger than a specified area. However, since the slope of the noncumulative power law is near unity, its integral or sum will be logarithmic. This is true of most models that exhibit self-organized criticality, since the slopes are generally near unity using a noncumulative frequency–area distribution.

Instead of converting the model results from a noncumulative to a cumulative distribution, we present the frequency–area data for landslides in a noncumulative form. This could be done by 'binning' the data; however, there would be ambiguities (for example, whether the bin size is in linear or logarithmic coordinates). Therefore, in order to compare the

(noncumulative) sandpile model results with actual landslides, we use a derivative method to convert a cumulative distribution of actual landslide areas to a noncumulative one.

We start with cumulative data, where N_{CL} is the number of landslides with area greater than A_L. We define a noncumulative distribution in terms of the negative of the derivative (i.e. the slope) of the cumulative distribution with respect to the area A_L. The value is negative, because the cumulative distribution is summed from the largest to the smallest values. The derivative, $\mathrm{d}N_{CL}/\mathrm{d}A_L$, is the slope of the best-fit line for a specified number of adjacent cumulative data points.

Malamud and Turcotte (1999) have considered four data sets for the frequency–area distributions of landslides. These authors derived the slopes, $\mathrm{d}N_{CL}/\mathrm{d}A_L$, of the cumulative data using five adjacent points and a least-squares fit in linear space. The negative of each slope is plotted as a function of the average of the five adjacent log A_L points in figure 3. The results suggest that the frequency–area distributions are similar despite different geographic settings and triggering mechanisms.

Earthquakes have long been recognized as a trigger for extensive landslides. The first data set (Harp and Jibson 1995) is a compilation of 11 000 landslides located over an area of 10 000 km^2 that were triggered by the January 17, 1994 Northridge, California earthquake. Harp and Jibson (1995) estimated that the inventory is nearly complete down to landslides of about 5 m on a side, below which a significant number may have been missed. The noncumulative frequency–area distribution is given in figure 3(a). The frequency–area distribution for large landslides is in good agreement with the power-law relation (1.1) with $\alpha \approx 2.3$. The observed frequency–area distribution flattens out for areas less than about 10^{-1} km^2, thus few landslides occur with small areas. Note that this change in the distribution occurs at an area that is an order of magnitude larger than the resolution of the catalogue. Therefore, it does not appear to be an artifact of completeness of the data set.

In the second data set, 3424 landslides with areas larger than 10^{-2} km^2 in the Akaishi Ranges, central Japan, have been compiled by Ohmori and Sugai (1995). In this region, landslides occur as a result of both heavy rainfall and strong earthquakes. It was estimated that the inventory is nearly complete for landslides with area greater than 10^{-2} km^2. The noncumulative frequency–area distribution is given in figure 3(b). The frequency–area distribution for large landslides is again in good agreement with the power-law relation (1.1) with $\alpha \approx 3.0$. Again the frequency–area distribution flattens out for small landslides.

In the third set, a set of landslide areas was mapped in the Challana Valley, Bolivia by Blodgett (1998). This is a relatively aseismic region of the Andes; therefore, the landslides are thought to have been hydrologically triggered during the wet season. The noncumulative frequency–area distribution is given in figure 3(c). The frequency–area distribution for large landslides is again in good agreement with the power-law relation (1.1) with $\alpha \approx 2.6$.

The fourth and final data set consists of the frequency–area distribution for 709 landslides in the Eden Canyon area, Alameda County, California (Nilsen *et al* 1975). The smallest landslide deposits mapped are about 50 m in dimension and the landslides range in age from tens to several hundred thousand years old. The noncumulative frequency–area distribution is given in figure 3(d); the frequency–area distribution for large landslides is again in good agreement with the power-law relation (1.1) with $\alpha \approx 3.3$.

All four data sets given in figure 3 exhibit similar behaviour. For the larger landslides, the noncumulative frequency–area distributions correlate well with the power-law relation (1.1) taking $\alpha \approx 2.3$–3.3. This slope is considerably larger than the sandpile model slope of $\alpha \approx 1.0$. It must be noted, however, that landslides have a depth as well as an area, so any comparison with the strictly two-dimensional sandpile model is only approximate. Nevertheless, all four data sets give reasonably good power-law correlations for the larger landslides. There are
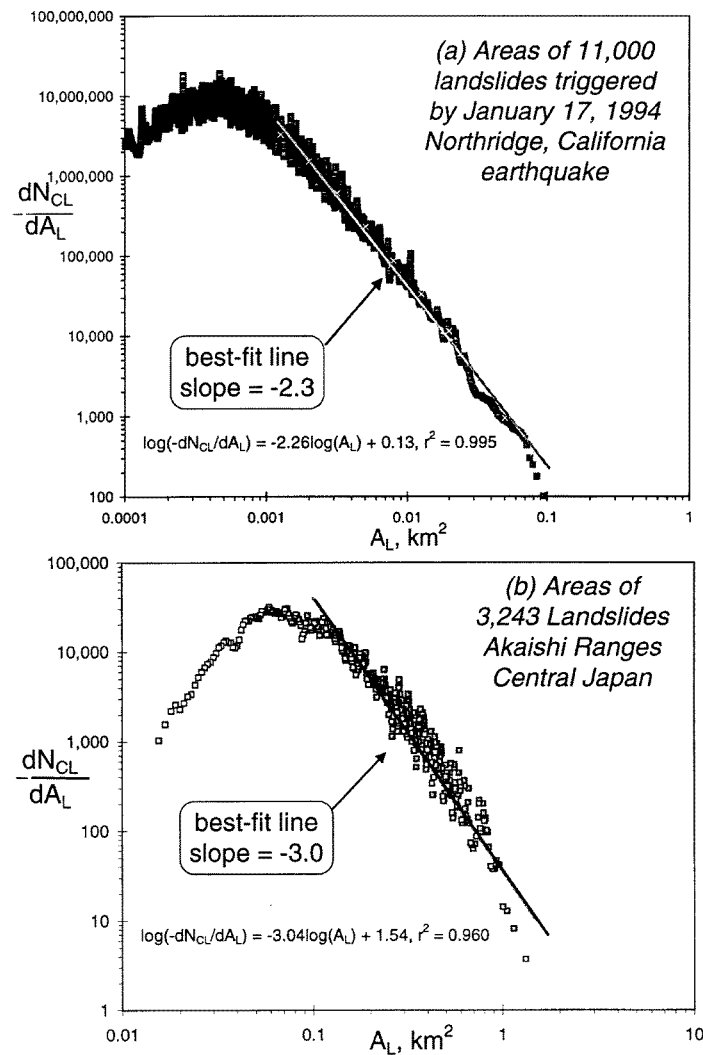
Figure 3. Noncumulative frequency–area distributions for actual landslides (Malamud and Turcotte 1999). Four examples are given: (*a*) 11 000 landslides triggered by the January 17, 1994 Northridge, California earthquake (Harp and Jibson 1995). (*b*) 3423 landslides in the Akaishi Ranges of central Japan (Ohmori and Sugai 1995). (*c*) 1130 landslides in the Challana valley, Yungas region, Eastern Cordillera, Bolivia (Blodgett 1998). (*d*) 709 landslides in the Eden Canyon area of Alameda county, California (Nilsen *et al* 1975). The noncumulative number of landslides, $-dN_{CL}/dA_L$, with area A_L, is given as a function of A_L. In each case a reasonably good correlation is obtained with the power-law relation (1.1) with $\alpha = 2.3$–3.3.

a number of similarities between the sandpile model and real landslides. Slope instabilities develop slowly and are eliminated in 'avalanches'. Power-law distributions are obtained. It is basically an arbitrary choice to decide whether landslides are an example of self-organized critical behaviour in nature.

In all four data sets, the frequency of occurrence of small landslides falls systematically below the predictions of the power-law correlation. This cannot be attributed to sampling problems since the fall-off occurs at landslide sizes considerably larger than the resolution
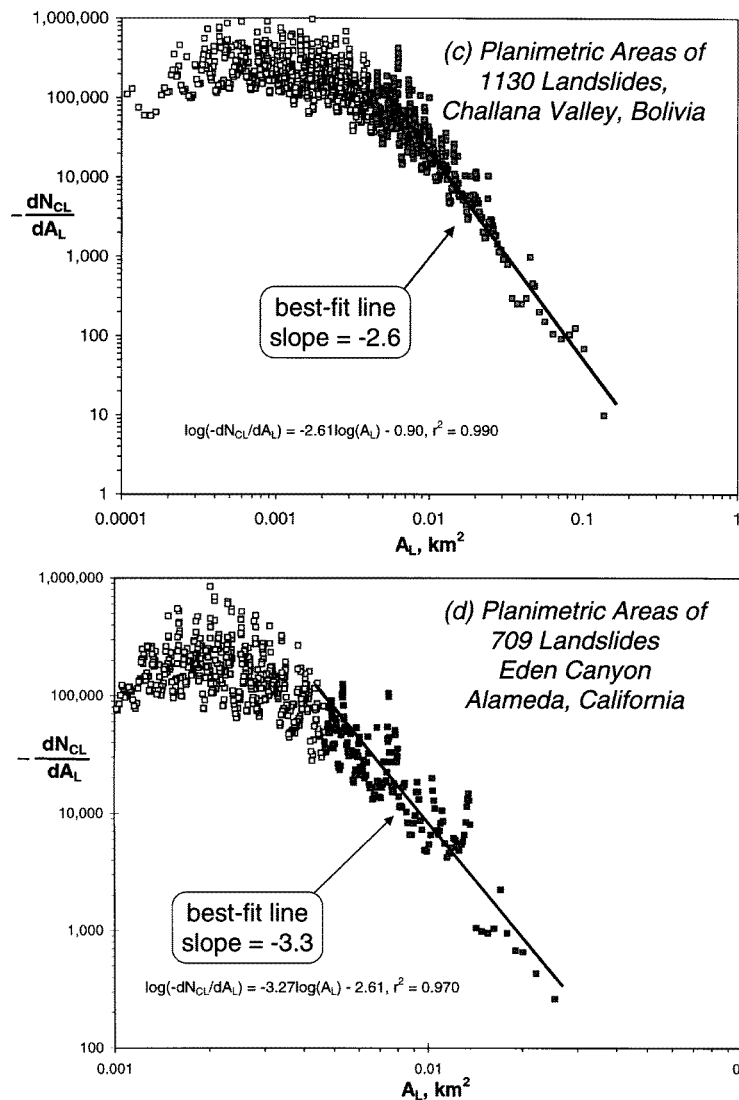
Figure 3. (Continued)

limits. The break in slope occurs at a scale of about 30 m, similar to that recognized in terms of river networks. River networks are believed to form at a scale of 30 m, so slope instabilities (landslides) related to rivers can only occur at larger scales.

Pelletier *et al* (1997) used observed power-law distributions of soil moisture in conjunction with a slope stability analysis to model the frequency–area distribution of landslides. In their model, landslides occur when a threshold shear stress dependent on cohesion, pore pressure, internal friction, and slope angle, is exceeded. Since cohesion, pore pressure, and internal friction are all primarily dependent on soil moisture, this implies a threshold dependence on soil moisture and slope angle. With soil moisture modelled as above and topography modelled as a Brownian walk, the cumulative frequency–area distribution of domains of shear stress greater than a threshold value is a power-law function of area with an exponent of -1.8 for

large landslide areas. This distribution is similar to that observed for landslides. The effect of strong ground motion from earthquakes lowers the shear stress necessary for failure, but does not change the frequency–area distribution of failed areas. This is consistent with observations. The fact that the surface upon which landslides occur is a self-affine fractal (Turcotte 1997), is an important difference between the sandpile model, laboratory studies, and real landslides. An alternative model for the power-law behaviour of landslides has been given by Hergarten and Neugebauer (1998).

2.4. Turbidites

Under some circumstances, sedimentary layers can be associated with landslides. Turbidite currents, a suspension of particles denser than the surrounding water, are associated with slumps (avalanches) off continental margins. Turbidity currents, triggered by a slump, can cover very large areas (hundreds of thousands of km^2) at high speeds (10–100 km h^{-1}). These events can be considered a natural analogue for sand slides, and thus the sandpile model considered above. The lithologic product of a turbidity current is a turbidite, each deposit representing a distinct event (slump). Each turbidite is composed of a general upward gradation from coarse-grained sediments to fine-grained sediments, and individual turbidites are generally separated by well-defined bedding planes.

Several studies of the frequency–thickness distributions of turbidite deposits have been carried out. Rothman *et al* (1994) carried out direct measurements on an outcrop of the Kingston Peak Formation near the southern end of Death Valley, California. Their results are given in figure 4(*a*), where the cumulative number of layers with thickness greater than h, N_c, is given as a function of h. Good agreement with the power-law (fractal) relation

$$N_c \sim h^{-D} \tag{2.3}$$

is obtained by taking $D = 1.39$. Rothman *et al* (1994) associated the observed power-law distribution of turbidite deposits with the power-law distribution of sandpile model avalanches. Hiscott *et al* (1992) have studied a volcanoclastic turbidite deposit in the Izu–Bonin forearc basin off the shore of Japan. Layer thicknesses were obtained from formation-microscanner images from well logs in the middle to upper Oligocene part of the section. Results for two DSDP (Deep Sea Drilling Project) holes located 75 km apart are given in figure 4(*b*); a good correlation with (2.3) is obtained by taking $D = 1.12$.

It is interesting to note that the fractal dimensions (power-law exponents) of the thickness statistics given in figure 4 are greater than one. Because this is a one-dimensional set, the fractal dimension would be expected to be in the range $0 < D < 1$. The reason for this is that the distribution will diverge as $h \to 0$. The Cantor set is a specific example of such a fractal distribution. Thus, the observed distributions are not strictly fractal. However, real distributions have both upper and lower cutoffs on the range of validity of (2.3). Thus, for natural distributions D need not be restricted to values less than one. This kind of ambiguity also arises in any association of natural phenomena with self-organized criticality.

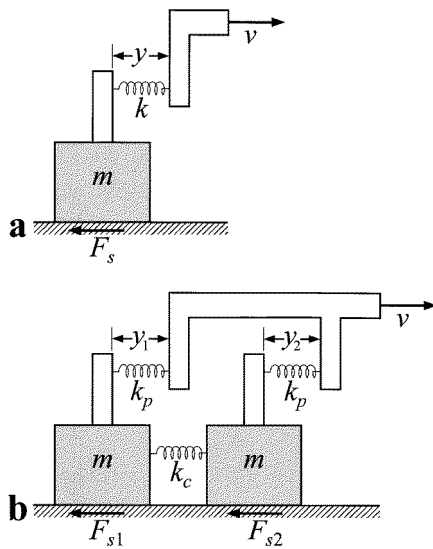## 3. Slider-block model

3.1. Chaotic behaviour

Slider-block models have also been said to exhibit self-organized critical behaviour. These models are considered to be simple analogues for the behaviour of faults in the Earth's crust. The simplest example, given in figure 5(*a*), is a single slider-block of mass m pulled over a surface by a spring constant k attached to a constant velocity v driver plate. The interaction of
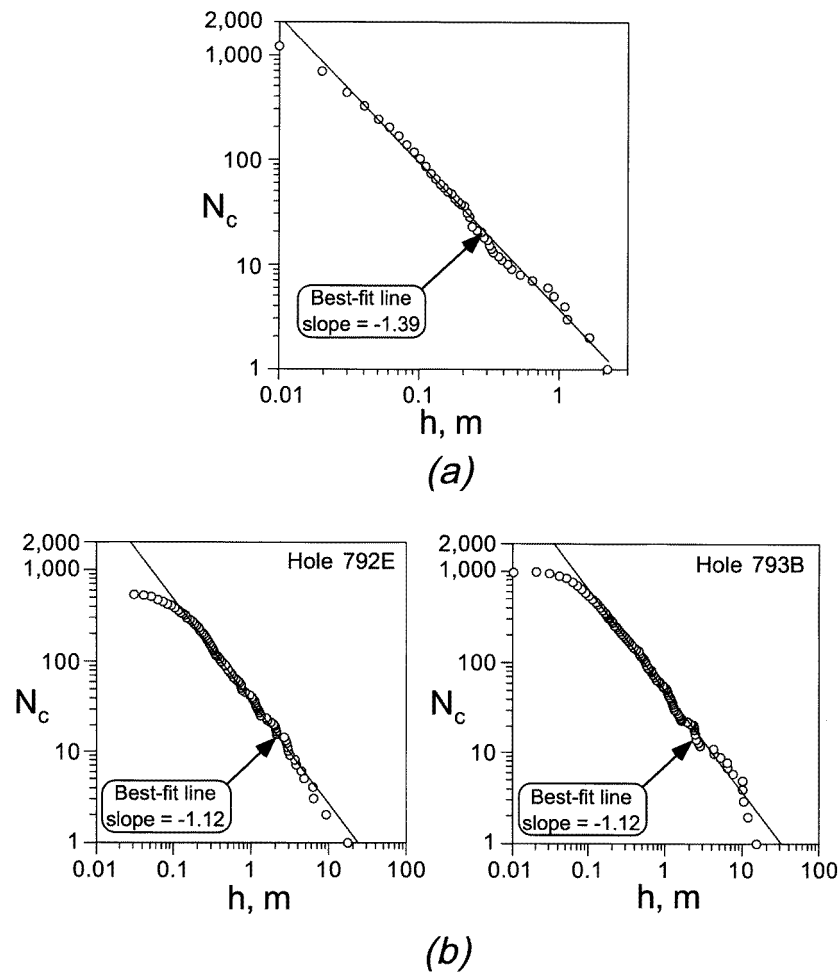
Figure 4. Cumulative frequency–thickness distributions for turbidite sequences of sedimentary layers. (*a*) Kingston Peak Formation near the southern end of Death Valley, California (Rothman *et al* 1994). (*b*) Izu–Bonin forearc basin off the shore of Japan (Hiscott *et al* 1992). Both sets of authors attribute the roll-off for thin layers to loss of resolution. In each case, N_C the number of beds with thickness greater than h is plotted as a function of h. The straight-line correlations with the power-law relation (2.3) give $D = 1.39$ for (*a*) and $D = 1.12$ for (*b*).

the block with the surface is controlled by friction. Many friction laws have been proposed; the simplest is the static–dynamic friction law. If $v = 0$ the static frictional force is F_s, if $v \neq 0$ the dynamic frictional force is F_d. If $F_s > F_d$, stick–slip behaviour is obtained and the motion of the block is made up of periodic slip events.

The behaviour of a pair of slider blocks was studied in detail by Huang and Turcotte (1990a, 1992). This model is illustrated in figure 5(*b*) and the equations of motion for the two blocks were solved simultaneously. Solutions were governed by two parameters, the stiffness of the system $\alpha = k_c/k_p$ (k_c the spring constant of the connector spring and k_p the spring constant of the puller springs) and the ratio of static to dynamic friction $\Phi = F_s/F_d$. For some values of these parameters, deterministic chaos was found. Chaotic behaviour requires some asymmetry in the problem, i.e. $F_{s1} \neq F_{s2}$. The period-doubling route to chaos was observed

Figure 5. Illustration of the slider-block model. (*a*) A single block of mass m is pulled over a surface by a constant-velocity v driver plate. The plate is connected to the block by a spring with spring constant k. The motion is restricted by a frictional force F_s. (*b*) Two blocks with mass m are pulled over a surface. The two masses are connected by a spring with spring constant k_c. Each mass is connected to the driver plate with spring constant k_p.
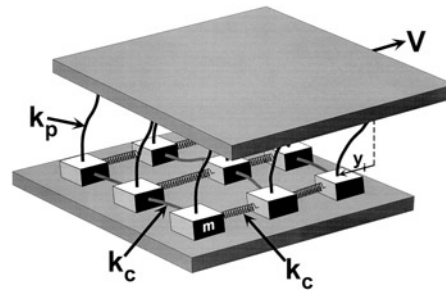
Figure 6. Illustration of the two-dimensional slider-block model. An array of blocks, each with mass m, is pulled across a surface by a driver plate at a constant velocity, V. Each block is coupled to the adjacent blocks with either leaf or coil springs (spring constant k_c), and to the driver plate with leaf springs (spring constant k_p).

with positive values of the Lyapunov exponent in the chaotic regions. The behaviour of the pair of slider blocks is very similar to the behaviour of the logistic map (May 1976).

A modification of this model is to allow only one block to slip at a time. The first block to become unstable is allowed to complete its harmonic motion before the stability of the second block is considered; if the second block is then unstable, it is allowed to slip before the motion of the driver plate is updated. This is a cellular-automata model. Extensive studies using this model were carried out (Narkounskaia and Turcotte 1992, Narkounskaia *et al* 1992) and these showed that its behaviour was essentially identical to the results obtained when both blocks were allowed to slip simultaneously.

The chaotic behaviour of the low-dimensional Lorenz equations (Lorenz 1963) is now accepted as evidence that the behaviour of the atmosphere and oceans is chaotic. Similarly, the chaotic behaviour of a pair of slider blocks is evidence that earthquakes exhibit chaotic behaviour (Huang and Turcotte 1990b).

3.2. Self-organized critical behaviour

The slider-block model with a pair of slider blocks considered above can be extended to include large numbers of slider blocks. Multiple slider-block simulations were first considered by Burridge and Knopoff (1967). Laboratory studies were carried out on a linear array of slider blocks pulled from one end. Large slip events were quasi-periodic and the smaller slip events satisfied a power-law dependence of cumulative number of events on size. Otsuka (1972) obtained power-law frequency–size statistics for a two-dimensional array of 2000 slider blocks using an electrical analogue without dynamic friction. Other early studies were also carried

out (Dietrich 1972, Cohen 1977, Rundle and Jackson 1977).

The standard multiple slider-block model consists of a square array of slider blocks as illustrated in figure 6. Each block with mass m is attached to the driver plate with a driver spring, spring constant k_p. Adjacent blocks are attached to each other with connector springs, spring constant k_c. A block remains stationary as long as the net force on the block is less than the static resisting force, F_s. This static stability criteria requires that

$$k_p x_{i,j} + k_c(x_{i+1,j} + x_{i-1,j} + x_{i,j+1} + x_{i,j-1} - 4x_{i,j}) < F_s \qquad (3.1)$$

with $x_{i,j}$ the position of block (i, j) in the array. When the stability criteria is violated the block begins to slip and its motion is given by

$$m \frac{d^2 x_{i,j}}{dt^2} + k_p x_{i,j} + k_c(x_{i+1,j} + x_{i-1,j} + x_{i,j+1} + x_{i,j-1} - 4x_{i,j}) = F_d \qquad (3.2)$$

where F_d is the dynamic frictional force between the block and the surface when the block is moving, and t is time in the slider-block model.

It is convenient to introduce the nondimensional variables

$$\tau = t \left(\frac{k_p}{m}\right)^{1/2}, \qquad X_{i,j} = \frac{k_p x_{i,j}}{F_s}, \qquad \Phi = \frac{F_s}{F_d}, \qquad \alpha = \frac{k_c}{k_p}. \qquad (3.3)$$

The stability condition (3.1) becomes

$$X_{i,j} + \alpha(X_{i+1,j} + X_{i-1,j} + X_{i,j+1} + X_{i,j-1} - 4X_{i,j}) < 1 \qquad (3.4)$$

and the equation of motion of a block becomes

$$\frac{d^2 X_{i,j}}{d\tau^2} + X_{i,j} + \alpha(X_{i+1,j} + X_{i-1,j} + X_{i,j+1} + X_{i,j-1} - 4X_{i,j}) = \Phi^{-1}. \qquad (3.5)$$

Two parameters determine the behaviour of the system: Φ, the ratio of static to dynamic friction, and $\alpha = k_c/k_p$, the stiffness of the system. For very soft systems, $\alpha \to 0$, the blocks exhibit stick–slip behaviour independently. For very stiff systems, $\alpha \to \infty$, the array of blocks behaves as a single block.

Carlson and Langer (1989a, b) considered long linear arrays of slider blocks with each block connected by springs to the two neighbouring blocks and to a constant-velocity driver. They used a velocity-weakening friction law and considered up to 400 blocks. Slip events involving large numbers of blocks were observed, the motions of all blocks involved in a slip event were coupled, and the applicable equations of motion had to be solved simultaneously. Because of the strong similarities, these are often known as molecular-dynamics simulations. Although the system is completely deterministic, the behaviour was apparently chaotic. Noncumulative frequency–size statistics were obtained for slip events. The smaller events obeyed a power-law (fractal) relationship with a slope near unity, but there were an anomalously large number of large events that included all the slider blocks. The observed behaviour was characteristic of self-organized criticality. The input in this model was the constant motion of the driver plate. The output or 'avalanches' were the slip events, with a power-law frequency–size distribution.

Nakanishi (1990, 1991) studied multiple slider-block models using the cellular automata approach. A linear array of slider blocks was considered but only one block was allowed to move in a slip event. The slip of one block could lead to the instability of either or both of the adjacent blocks, which would then be allowed to slip in a subsequent step or steps, until all blocks were again stable. Brown *et al* (1991) proposed a modification of this model involving a two-dimensional array of blocks. The use of the cellular automata approach greatly reduces the complexity of the calculations.
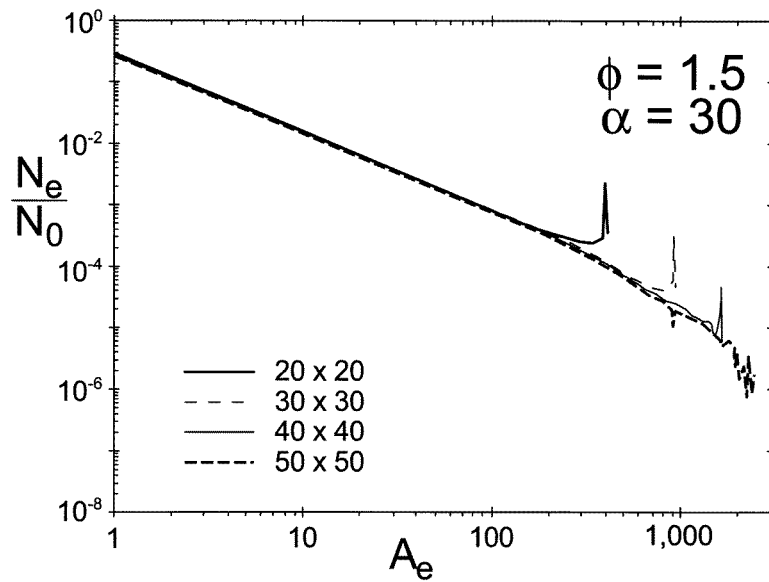
Figure 7. The ratio of the number of slip events, N_e, with area A_e, to the total number of slip events N_0, is plotted against A_e (Huang *et al* 1992). Results are given for systems with stiffness $\alpha = k_c/k_p = 30$, friction $\Phi = F_s/F_d = 1.5$, and grid sizes 20×20, 30×30, 40×40, and 50×50. The peaks at $A_e = 400$, 900, and 1600, correspond to catastrophic slip events involving the entire system.

Huang *et al* (1992) carried out many simulations on a square array of blocks using static–dynamic friction and a cellular-automata approach. Their noncumulative frequency–area distribution statistics for model slip events are given in figure 7. The number of slip events per time step with area A_e, N_e/N_0, is given as a function of A_e. Results are given for a stiffness $\alpha = 30$, friction $\Phi = 1.5$ and grid sizes, 20×20, 30×30, 40×40, and 50×50. There is agreement with the power-law relation (1.1) with power-law exponent $\alpha \approx 1.3$. For stiff systems, $\alpha = k_c/k_p$ large, the entire grid of slider blocks is strongly correlated and large slip events including all the blocks occur regularly. These are the peaks for $A_e = 400$, 900, and 1600, illustrated in figure 7. For soft systems, $\alpha = k_c/k_p$ relatively small, no large events occur.

There are strong similarities between the behaviour of the sandpile model and the slider-block model. In both cases smaller slip events have a noncumulative power-law frequency–area distribution with similar power-law exponents, $\alpha \approx 1.0$–1.3. Whereas the sandpile model is stochastic in the selection of boxes, the slider-block model is fully deterministic. The slider-block model provides a bridge between chaotic behaviour (two slider blocks) and self-organized critical behaviour (large numbers of slider blocks). Adjacent solutions for the chaotic behaviour of a pair of slider blocks diverge exponentially. Adjacent solutions for large numbers of slider blocks have a power-law divergence.

Many papers have been written reporting simulations based on the slider-block model (Carlson 1991a, b, Carlson *et al* 1991, 1993a, b, Feder and Feder 1991, Matsuzaki and Takayasu 1991, Vasconcelos *et al* 1991, 1992, Crisanti *et al* 1992, Christensen and Olami 1992a, b, Ito 1992, McCloskey and Bean 1992, 1994, Olami and Christensen 1992, Shaw *et al* 1992, Sornette 1992, Cowie *et al* 1993, Ding and Lu 1993, de Sousa Vieira *et al* 1993, Knopoff *et al* 1993, McCloskey 1993, McCloskey *et al* 1993, Schmittbuhl *et al* 1993, 1996,

Shaw 1993a, b, 1994, 1995, 1997, Espanol 1994, Lin and Taylor 1994, Lu *et al* 1994, 1998, Senatorski 1994, 1995, Xu and Knopoff 1994, Carlson and Swindle 1995, Ceva 1995, de Sousa Vieira 1995, 1996, Liu *et al* 1995, Middleton and Tang 1995, de Sousa Vieira and Lichtenberg 1996, Cartwright *et al* 1997, Leung *et al* 1997, 1998a, b, Lise and Stella 1998, Hainzl *et al* 1999). One extension was to consider a linear chain of slider blocks pulled at one end (de Sousa Vieira 1992); this is a model for a propagating rupture on a fault.

Models with far field interactions and no inertia have been considered (Rundle and Klein 1989, 1993, 1995, Rundle and Brown 1991, Olami *et al* 1992, Rundle 1993, Grassberger 1994, Rundle *et al* 1996a, Ferguson *et al* 1998, Kinouchi *et al* 1998). Typically in these models a redistribution occurs when the stress on a block reaches a critical value. This stress is redistributed to a number of neighbouring blocks (not just nearest neighbours) in a specified way. These neighbours may subsequently fail. In general, there is a noise added to specified values. These models can be discussed in terms of a spinodal phase change. It has been found that the distribution of energies in the springs in this class of models is Boltzmann (Rundle *et al* 1995, 1996c, 1997).

There is evidence that cellular automata versions of slider-block models behave systematically differently than the molecular dynamics versions. Both generate power-law distributions of small events but the molecular dynamic simulations appear to generate a class of larger events not found in the cellular automata simulations. In order to study this difference studies have been carried out on a multiple slider-block model with no driver plate and no dynamic friction (Morein *et al* 1997, Morein and Turcotte 1998). Energy is conserved and the static friction acts as a nonlinear switch. In the cellular automata approach a Boltzmann distribution of energies was found but in the molecular dynamics approach normal-mode oscillations were found. These oscillations strongly resembled the oscillons observed in vertically vibrating granular layers (Umbanhowar *et al* 1996).

Studies have also been carried out on the predictability of the major slip events in slider-block models with mixed results (Bak *et al* 1994, Pepke and Carlson 1994, Pepke *et al* 1994, Rundle *et al* 1996b, Zhang *et al* 1996). Slider-block models have been reviewed by Carlson *et al* (1994) and Turcotte (1997).

3.3. Earthquakes

Since the concept of self-organized criticality was first introduced, earthquakes have been identified as an example of this phenomena in nature (Bak and Tang 1989). Earthquakes occur primarily in the brittle upper crust of the Earth at depths of less than 20 km. Most earthquakes occur at or near the boundaries of the tectonic plates, but a few earthquakes occur within plate interiors. Stress is added to the crust slowly due to the tectonic motion of the plates and is relieved rapidly in earthquakes (avalanches). The crustal stress oscillates about an equilibrium value.

For over 50 years, it has been accepted that earthquakes universally obey Gutenberg–Richter scaling; the cumulative number of earthquakes per year in a region with magnitudes greater than m, $\dot{N}_{CE}$, is related to m by (Gutenberg and Richter 1954)

$$\log \dot{N}_{CE} = -bm + \log \dot{a} \tag{3.6}$$

where the constant b is known as the b-value and has a near-universal value $b = 0.90 \pm 0.15$ (Evernden 1970). The constant $\dot{a}$ is a measure of the intensity of the regional seismicity.

When (3.6) is expressed in terms of the earthquake rupture area, A_E, instead of earthquake magnitude, this relation becomes a power law (Aki 1981)

$$\dot{N}_{CE} \sim A_E^{-b} \tag{3.7}$$
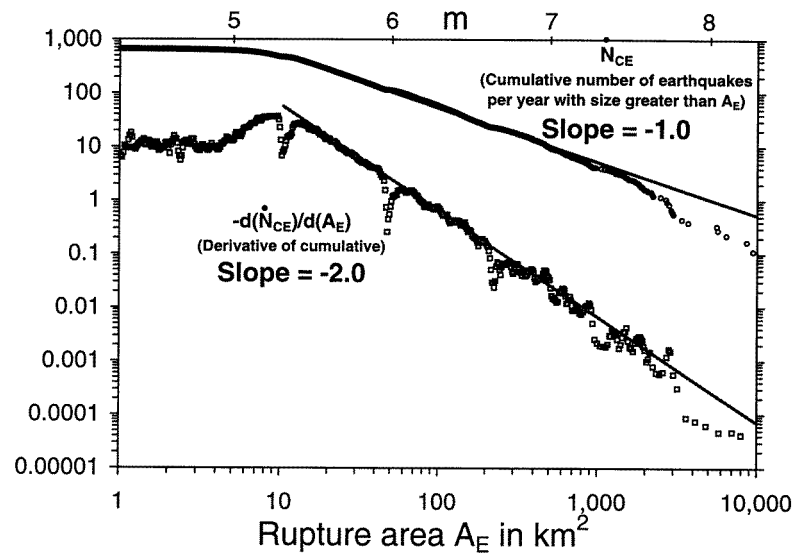
Figure 8. Worldwide cumulative, $\dot{N}_{CE}$, and noncumulative, $-\mathrm{d}\dot{N}_{CE}/\mathrm{d}A_E$, number of earthquakes per year with rupture areas greater than A_E as a function of A_E. These data are from the Harvard Centroid-Moment Tensor Data Base (1997) for the years (1977–94). Earthquake seismic moments have been converted to rupture areas. The equivalent magnitudes, m, are also given.

which is very similar to (1.1), except that (3.7) is based on cumulative statistics and (1.1) is based on noncumulative statistics.

We first consider the worldwide number of earthquakes per year from the Harvard Centroid-Moment Tensor Data Base (1997) for the period 1977–94. Both the cumulative number of earthquakes per year, $\dot{N}_{CE}$, with rupture area greater than A_E and the noncumulative number of earthquakes per year, $-\mathrm{d}\dot{N}_{CE}/\mathrm{d}A_E$, are given as a function of A_E in figure 8. The equivalent magnitudes, m, are also given in figure 8. The cumulative worldwide data per year correlate with (3.6) taking $b = 1.0$ and $\dot{a} = 10^8$ per year. The data given in figure 8 can be used to estimate the frequency of occurrence of earthquakes of various magnitudes on a worldwide basis. For example, about ten magnitude-seven earthquakes are expected each year and a single magnitude-eight earthquake can be expected in a year. As expected, the slopes of the cumulative and the noncumulative distributions differ by exactly one.

The deviation of the data from the Gutenberg–Richter law (3.6) at magnitudes less than $m = 5.2$ can be attributed to the resolution limits of the global seismic network. Regional studies indicate that good correlations are obtained down to at least $m = 2.0$ (Aki 1987). The deviation of the data from the Gutenberg–Richter law at magnitudes greater than $m = 7.5$ is more controversial (Scholz 1997). Clearly, there must be an upper limit to the size of an earthquake; but the deviations in figure 8 can be attributed either to a real deviation from the correlation line or to the small number of very large earthquakes in the relatively short time span considered. There is a physical basis for a change in scaling for large earthquakes (Pacheco *et al* 1992). The rupture zone of smaller earthquakes can be approximated by a circle of radius r, so that $r \sim A_E^{1/2}$. However, the depth of large earthquakes is confined by the thickness of the seismogenic zone, say about 20 km, whereas the length, l, can increase virtually without limit. Thus for large earthquakes, $l \sim A_E$. The transition would be expected to occur for $A_E^{1/2} \approx 25$ km or $m \approx 7$.

As we have shown, the models we have considered typically have good agreement with the noncumulative frequency–area power-law relation (1.1) taking $\alpha \approx 1.0$–3.0. The cumulative data shown in figure 8 are in good agreement with equation (3.7) with exponent $b \approx 1.0$. Bak and Tang (1989) pointed out the similarity in slopes between self-organized critical behaviour and earthquakes. However, the model data are noncumulative, and the earthquake data cumulative; therefore, the agreement must be considered fortuitous. The equivalent noncumulative frequency–area distribution of earthquake rupture areas would follow a power-law relation (1.1) with $\alpha \approx 2.0$. The power-law exponents for earthquakes are significantly higher than for the corresponding model (the slider-block model).

In order to further consider the applicability of the Gutenberg–Richter relation to seismicity we consider the frequency–magnitude distribution of earthquakes in southern California on a yearly basis using data obtained from the Southern California Seismographic Network (SCSN Catalog 1995). In figure 9, for each individual year between 1980–94, the cumulative number of earthquakes $\dot{N}_{CE}$ with magnitudes greater than m is plotted as a function of m. The period 1980–94 taken together results in the Gutenberg–Richter power-law relation (3.6) with $b = 1.05$ and $\dot{a} = 2.06 \times 10^5$ per year, shown as the solid straight lines in figures 9(*a*)–(*c*). In figure 9, there is generally good agreement between each individual year's data and the Gutenberg–Richter relation (solid straight line) for the period 1980–94. The exceptions can be attributed to the aftershock sequences of the 1987 Whittier, 1992 Landers, and 1994 Northridge earthquakes.

With aftershocks removed, the background seismicity in southern California illustrated in figure 9 is nearly uniform from year to year, and is not a function of time. Small earthquakes behave like a thermal background noise. This is observational evidence that the Earth's crust is continuously on the brink of failure (Scholz 1991). Further evidence for this comes from induced seismicity. Whenever the crust is loaded, whether in a tectonically active area or not, earthquakes are induced. Examples of loading include the filling of a reservoir behind a newly completed dam or the high-pressure injection of fluids in a deep well.

While there are important similarities between slider-block models and earthquakes there are also important differences. Slider-block models would be representative of a distribution of earthquakes on a single fault. However, the Gutenberg–Richter distribution of earthquakes is not associated with a single fault but with a hierarchy of faults. Small earthquakes occur on small faults and large earthquakes occur on large faults. The earthquakes included in the southern California data given in figure 9 occur over a broad zone with a width of about 200 km on a wide variety of faults associated with the San Andreas system.

There is extensive evidence that the distribution of faults in the crust is fractal (power-law). This has led to the suggestion (Sammis *et al* 1987) that comminution of the crust has led to a power-law distribution of tectonic blocks. The boundaries of these blocks are the power-law distribution of faults. Typically the cumulative number of faults with areas greater than A_E would satisfy (3.7) with $b \approx 0.8$.

A number of authors have considered the relationship between earthquakes and self-organized criticality (Sornette and Sornette 1989, Ito and Matsuzaki 1990, Sornette *et al* 1990, Bak and Chen 1995, Huang *et al* 1998). Although slider-block models are the primary basis for associating earthquakes with self-organized criticality, other models such as crack propagation (Chen *et al* 1991) and interface depinning (Paczuski and Boettcher 1996, Fisher *et al* 1997) have been proposed.

An important aspect of self-organized criticality relative to earthquakes is the implications for earthquake forecasting and prediction. Acceptance of the validity of the Gutenberg–Richter relation (3.6), and the constant rate of occurrence of small earthquakes illustrated in figure 9, implies that the observed frequency of occurrence of small earthquakes can be extrapolated
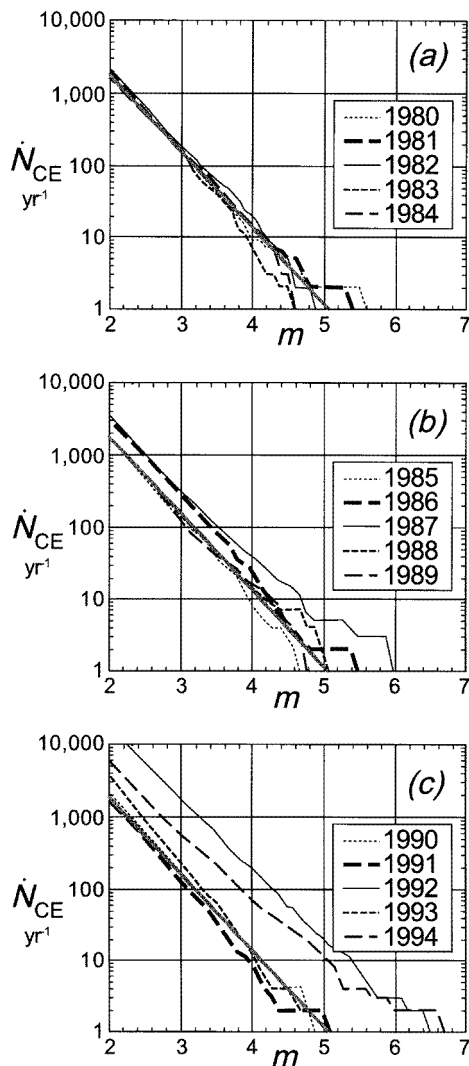
Figure 9. The cumulative number of earthquakes per year, $\dot{N}_{CE}$, occurring in southern California, with magnitudes greater than m as a function of m. Fifteen individual years are considered (SCSN Catalog 1995): (*a*) 1980–4; (*b*) 1985–9; (*c*) 1990–4. The heavy straight line in (*a*)–(*c*) represents the best fit to all data during 1980–94, the Gutenberg–Richter relation (3.6) with $b = 1.05$ and $\dot{a} = 2.06 \times 10^5$ per year. The larger number of earthquakes in 1987, 1992, and 1994 can be attributed to the aftershocks of the Whittier, Landers, and Northridge earthquakes, respectively. If aftershocks are excluded, the background seismicity in southern California is nearly uniform in time.

to estimate the recurrence frequencies of larger earthquakes. This is routinely done and is a primary basis for published maps of the earthquake hazard (Turcotte 1999).

A Russian group developed pattern recognition algorithms to provide intermediate range predictions of earthquakes (Keilis-Borok 1996). A number of successful predictions have been made. The algorithms use increased intermediate level seismicity and changes in aftershock statistics to make the predictions. These changes are observed over relatively large areas so that they imply the long-range interactions associated with critical phenomena. It should be emphasized, however, that this approach is controversial (Main 1996, Geller 1997, Geller *et al* 1997, Kagan 1997, Leary 1997). Bufe and Varnes (1993) have shown that there is a systematic power-law increase in seismic activity before a major earthquake. This increase is restricted to intermediate size events and does not extend to small events. Bowman *et al* (1998) have carried out a systematic study of the optimum correlation length over which this precursory activation occurs. They find the radius of the optimum region is about ten times the radius of the subsequent earthquake rupture.

4. Forest-fire model

4.1. Cellular-automata model

Although the forest-fire model (e.g. Bak *et al* 1992, Drossel and Schwabl 1992a, b, Henley 1993) was not the first model that was associated with self-organized criticality, it is probably the most illustrative. The forest-fire model we consider consists of a square grid of sites, with G the size of the grid. At each time step, a model tree is dropped on a randomly chosen site; if the site is unoccupied, the tree is planted. The sparking frequency, f_s, is the inverse number of attempted tree drops on the square grid before a model match is dropped on a randomly chosen site. If $f_s = \frac{1}{100}$, there have been 99 attempts to plant trees (some successful, some unsuccessful) before a match is dropped at the 100th time step. If the match is dropped on an empty site, nothing happens. If it is dropped on a tree, the tree ignites and a model fire consumes that tree and all adjacent (nondiagonal) trees.

As a specific example, consider the 10×10 grid ($G = 100$) illustrated in figure 10. Each grid site is identified by row and column as shown. The sparking frequency is $1/f_s = 5$; four trees are planted (or attempts to plant are made) before a spark is dropped. Sites are randomly chosen. The beginning configuration has six trees, and is the result of running the simulation for some time so that a quasi-equilibrium state is established. In steps 1–4, trees are dropped on the randomly chosen sites '54', '71', '85' and '19'. In the first three steps, the sites are empty, so a tree is planted. In step 4, site '19' is already occupied, so nothing happens. In step 5, a spark is dropped on a site '99', but it is unoccupied so nothing happens. In steps 6–9, four trees are planted on sites '17', '81', '43' and '68'. Finally, in step 10, a spark is dropped on site '54' which is occupied by a tree. This tree 'burns' along with the adjacent trees on sites '44' and '43' and are eliminated from the grid. The tree in site '35' does not burn because, although adjacent, it is diagonal to the sites being consumed by the fire. This 'forest fire' has a size $A_F = 3$, since three trees are burned.

For large time intervals, the number of trees lost in 'fires' is approximately equal to the number of trees planted. However, the number of trees on the grid will fluctuate. The frequency–area distribution of 'fires' is a statistical measure of the behaviour of the system. This model is probabilistic (stochastic) in that the sites are chosen randomly. It is a cellular-automata model in that only nearest-neighbour trees are ignited by a 'burning' tree. In terms of the definition of self-organized critical behaviour, the steady-state input is the continuous planting of trees. The avalanches in which trees are lost are the 'forest fires'. A measure of the state of the system is the fraction of sites occupied by trees. This 'density' fluctuates about a 'quasi-equilibrium' value.

Having specified the size of the square grid, G, and the sparking frequency, f_s, a simulation is run for N_S time steps and the number of fires N_F with area A_F is determined. The area, A_F, is the number of trees that burn in a fire. Examples of four typical fires during a run are given in figure 11. In these examples the grid size is 128×128 ($G = 16\,384$), $1/f_s = 2000$, and fires with $A_F = 5, 51, 506,$ and 5327 trees are illustrated. Figure 11(*d*) is an example of a special class of forest fire that spans the grid.

The noncumulative frequency–area distributions for the model forest fires are given in figures 12 and 13. The number of fires per time step with area A_F, N_F/N_S, is given as a function of A_F. In figure 12, results are given for a grid size 128×128 and three sparking frequencies, $1/f_s = 125, 500,$ and 2000. In figure 13, results are given for a sparking frequency $1/f_s = 500$ and three grid sizes, 64×64, 128×128, and 256×256. In all cases the smaller fires correlate well with the power-law relation (1.1) with $\alpha = 1.0$–1.2.

These results clearly indicate the finite-size effect of the grid. If f_s is large, the frequency–
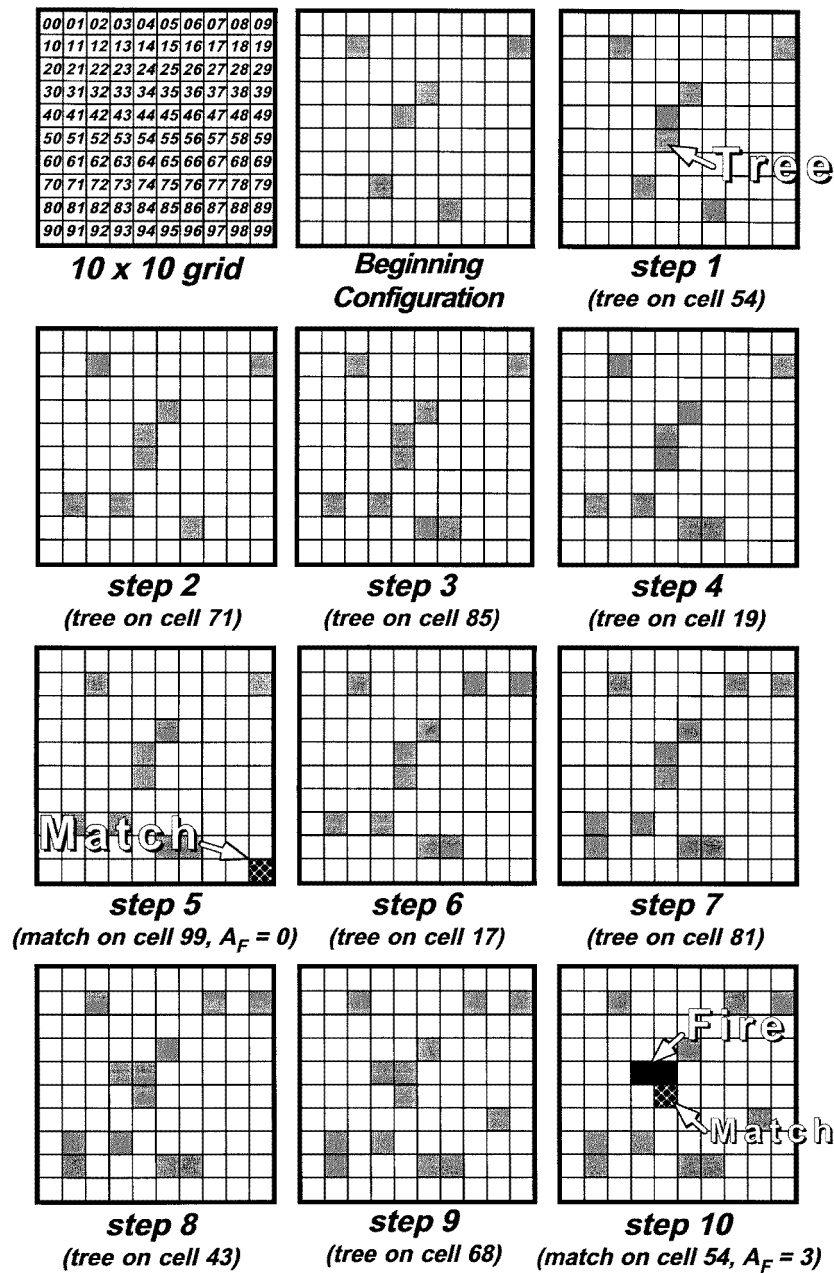
Figure 10. Illustration of the forest-fire model. A 10 × 10 grid is considered with sparking frequency $1/f_s = 5$. White boxes are unoccupied sites. Lightly shaded boxes are sites occupied by one tree. Match drops are indicated by a criss-cross pattern. Black boxes are the forest fires. Ten time steps are shown. The model 'fire' at step 10 consumes three trees.

area distribution begins to deviate significantly from a straight line, such that there is an upper termination to the power-law distribution. In figure 12, the deviation begins for $1/f_s = 125$ and $G = 128 \times 128$ at $A_F \approx 1000$. In figure 13, the deviation begins for $1/f_s = 500$ and
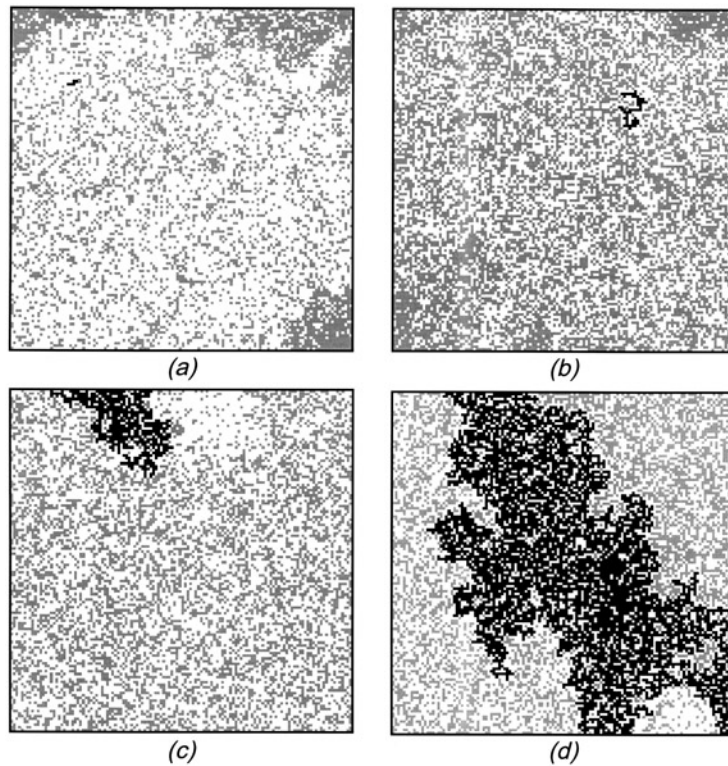
Figure 11. Four examples of typical model forest fires are given for a 128×128 grid with sparking frequency $1/f_s = 2000$. The heavily shaded regions are forest fires. The lightly shaded regions are unburned forest. The white regions are unoccupied sites. The areas A_F of the four forest fires are (*a*) 5, (*b*) 51, (*c*) 505 and (*d*) 5327 trees. The largest forest fire is seen to span the entire grid.

$G = 256 \times 256$ at $A_F \approx 4000$. It is also seen that large forest fires become dominant when the sparking frequency is very small. This is easily explained on physical grounds. This transition is clearly illustrated in figure 12. With large sparking frequencies (for example $1/f_s = 125$), trees burn before large clusters can form. For small sparking frequencies (for example $1/f_s = 2000$) clusters form that span the entire grid before ignition occurs.

In figure 13, with a large grid (for example 256×256), trees burn before large clusters can form. However, for a small grid (for example 64×64) clusters form that span the entire grid before ignition occurs. For very small firing frequencies or very small grid sizes, there will be very few fires that form with small values of area, A_F. The grid will become very full before a match sparks a fire. The areas of the fires will all involve a large number of trees, and in most cases the fires will span the grid.

Comprehensive studies of the forest-fire model have been given by Mossner *et al* (1992) and by Clar *et al* (1996, 1999). Many variations on the basic 'forest-fire' model given above have been studied. Simulations have been carried out in one to six dimensions (Christensen *et al* 1993), other one-dimensional studies have been undertaken (Drossel *et al* 1993, 1994a, Paczuski and Bak 1993, Honecker and Peschel 1996), phase transitions have been considered (Clar *et al* 1997), immune 'trees' have been introduced (Drossel and Schwabl 1993b, Albano 1994, 1995), the renormalization group approach has been applied (Loreto *et al* 1995a, b, 1996) and a variety of other studies have been carried out (Grassberger and Kantz 1991, Drossel and
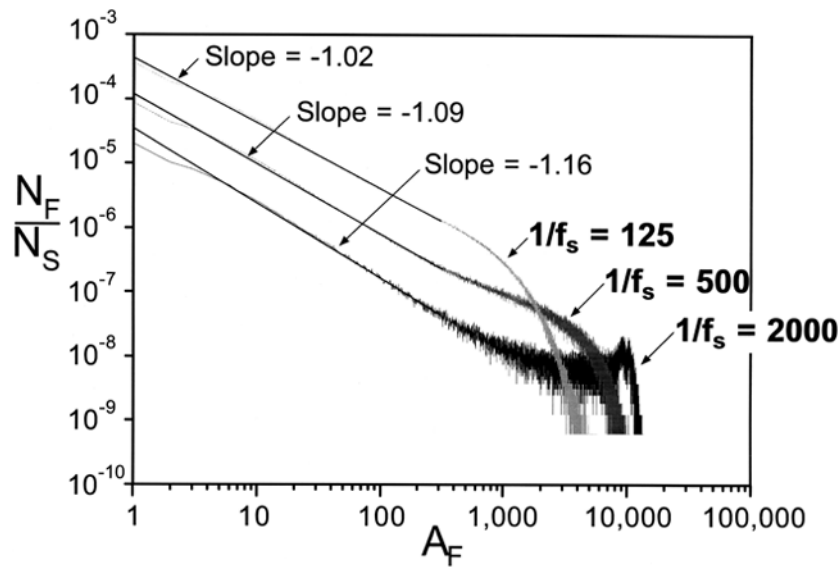
Figure 12. Noncumulative frequency–area distributions of model forest fires with constant grid size and changing sparking frequency. The number of fires per time step with size A_F, N_F/N_S, is given as a function of A_F, where A_F is the number of trees burned in each fire. Results are given for grid size 128×128 and sparking frequencies, $1/f_s = 125, 500, 2000$. For each f_s the model was run for $N_S = 1.638 \times 10^9$ time steps. The small and medium fires correlate well with the power-law relation (1.1) taking $\alpha = 1.02$–1.18. The finite grid size effect can be seen at the smallest sparking frequency, $1/f_s = 2000$. At $1/f_s = 2000$ fires begin to span the entire grid.

Schwabl 1993a, 1994, Grassberger 1993, Clar *et al* 1994, 1995, Strocka *et al* 1995, Drossel 1996, 1997, Broker and Grassberger 1997, Honecker and Peschel 1997).

4.2. Forest and wild fires

An obvious application of the forest-fire model is to actual forest and wild fires (Malamud *et al* 1998). From this study, four forest-fire and wildfire data sets from the United States and Australia are given in figure 14. The first data set includes 4284 fires on US Fish and Wildlife Service land during the period 1986–95. The second data set includes the areas of 120 forest fires as interpreted from tree rings for the western United States for the period 1155–1960. The third data set includes the areas of 164 fires in Alaskan Boreal Forests during 1990–91. The fourth data set includes 298 fires in the Australian Capital Territory during 1926–91. The data sets come from a wide variety of geographic regions with different vegetation types and climates. In each case, the cumulative number of fires per year, $\dot{N}_{CF}$, with area greater than A_F has been converted to a noncumulative distribution using the technique described in section 2.3. The results given in figure 14 correlate well with the power-law relation (1.1) taking $\alpha = 1.3$–1.5.

The actual forest fires (figure 14) have good power-law distributions over many orders of magnitude, consistent with the model data (figures 12 and 13). However, the model data have power-law exponents ($\alpha = 1.0$–1.2) that are somewhat less than those calculated for the actual data. The model is in reasonable, but not exact, agreement with the actual data.

Considering the many complexities of the initiation and propagation of forest fires and wildfires it is remarkable that the frequency–area statistics are very similar under a wide variety
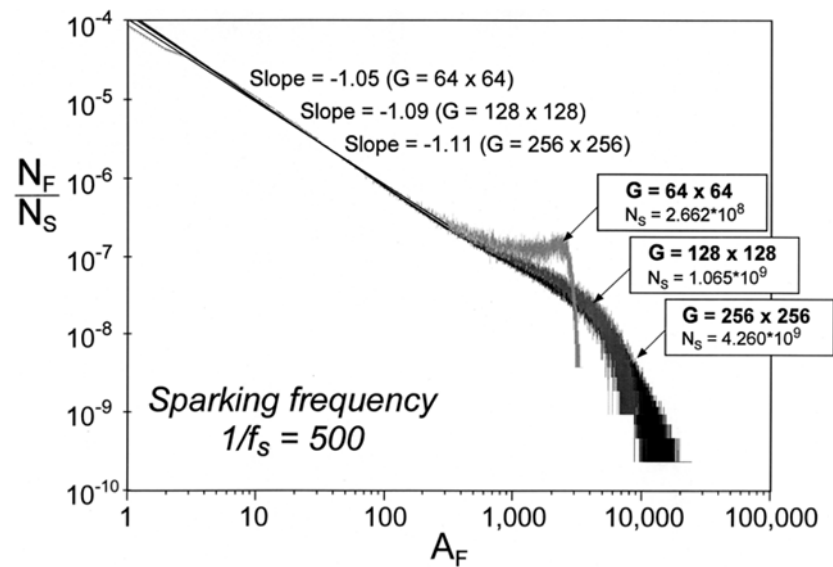
Figure 13. Noncumulative frequency–area distributions of model forest fires with changing grid size and constant sparking frequency. The number of fires per time step with size A_F, N_F/N_S, is given as a function of A_F where A_F is the number of trees burnt in each fire. Results are given for three grid sizes, $G = 64 \times 64$, 128×128, 256×256 and a constant sparking frequency, $1/f_s = 500$. The number of time steps, N_S, that the model was run for each grid size is noted.

of environments. The proximity of combustible material varies widely. The behaviour of a particular fire depends strongly on meteorological conditions. Fire-fighting efforts extinguish many fires. Despite these complexities, the application of the frequency–area distributions associated with the forest-fire model appears to be robust. Further confirmation of the applicability of the forest-fire model to real forests is the observation that clusters of trees in forests obey fractal (power-law) statistics (Sole and Manrubia 1995a, b). Another application of the forest-fire model has been to the spread of disease (Johansen 1994) and, in particular, to measles epidemics (Rhodes and Anderson 1996a, b, Rhodes *et al* 1997).

5. Criticality versus self-organized criticality

5.1. An inverse-cascade model

The behaviour of the forest-fire model can be understood using an inverse-cascade model. The one-dimensional forest-fire model has been discussed in terms of a cascade by Paczuski and Bak (1993). In the model presented here (Turcotte *et al* 1999) clusters of 'trees' are considered that contain $1, 2, 2^2, \ldots, 2^n$ trees. Single trees are introduced to the cascade and coalesce to form larger clusters. Fires burn clusters of all sizes, but significant numbers of trees are lost only in model fires that burn the largest clusters. There is a cascade of trees from smaller to larger clusters and this cascade gives a power-law frequency–size distribution of clusters. The loss of large clusters in fires terminates the cascade.

From figures 12 and 13 it is seen that the frequency–area distribution of the smaller model forest fires correlates well with the power-law relation (1.1) with exponent $\alpha = 1.0$–1.2. We
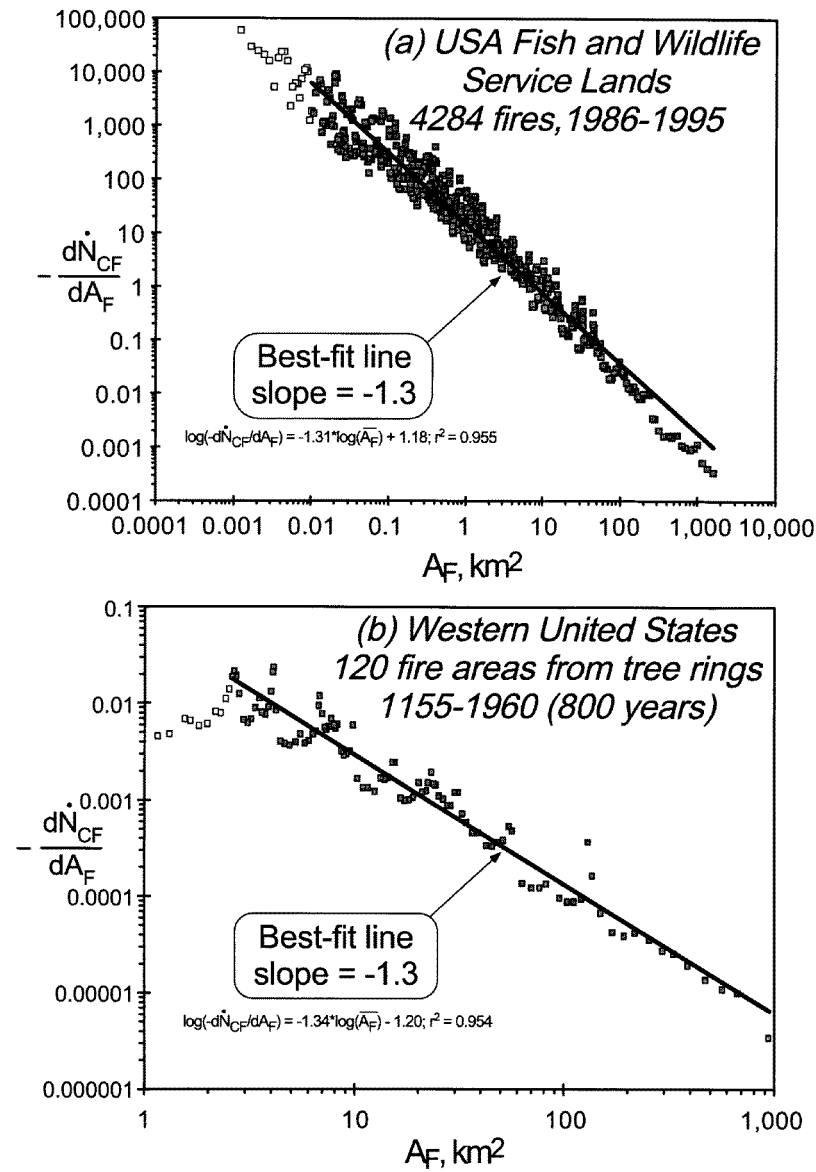
Figure 14. Noncumulative frequency–area statistics for actual forest fires and wildfires in the United States and Australia (Malamud *et al* 1998). Four examples are given: (*a*) 4284 fires on US Fish and Wildlife Service land during 1986–95 (National Interagency Fire Center 1996). (*b*) 120 fires in the western United States during 1155–1960, calculated from tree ring data (Heyerdahl *et al* 1994). (*c*) 164 fires in Alaskan Boreal Forests during 1990–91 (Kasischke and French 1995). (*d*) 298 fires in the Australian Capital Territory during 1926–91 (ACT Bush Fire council 1996). For each data set, the noncumulative number of fires per year, $-\mathrm{d}\dot{N}_{CF}/\mathrm{d}A_F$, with area A_F, is given as a function of A_F. In each case a reasonably good correlation over many decades of A_F is obtained by using the power-law relation (1.1) with $\alpha = 1.3$–1.5.

approximate this behaviour with $\alpha \approx 1$, giving

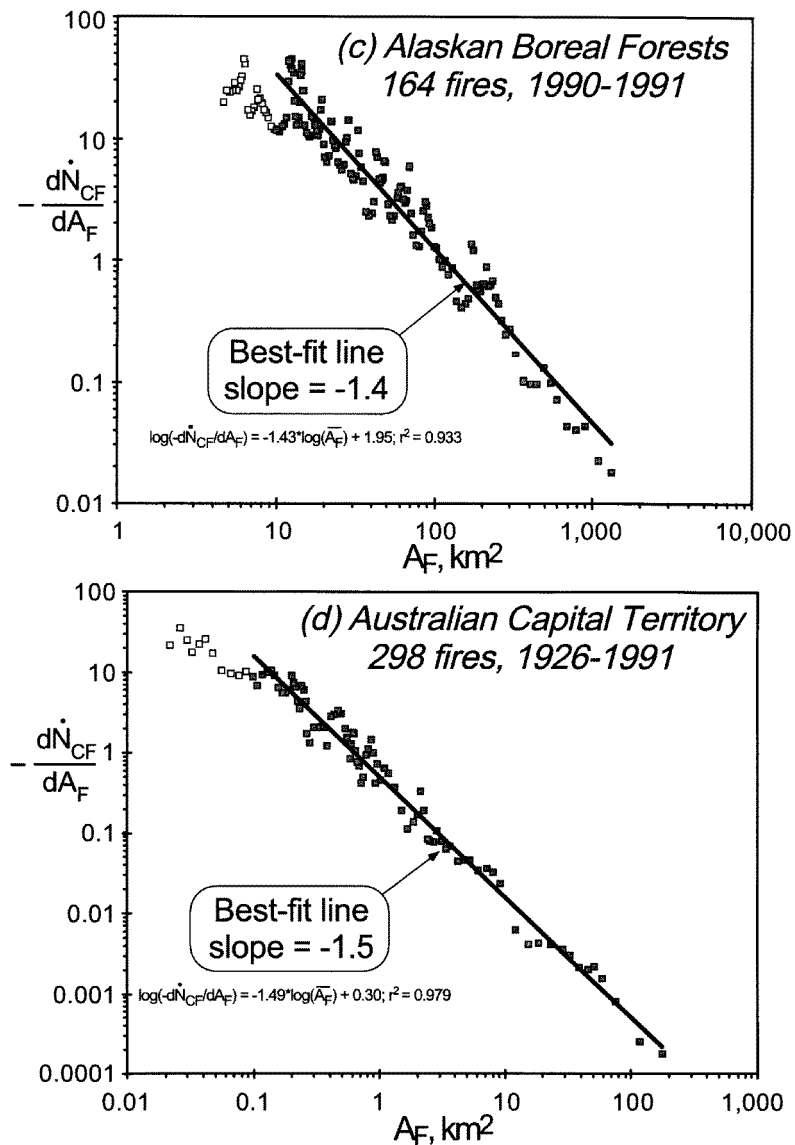$$\frac{N_f}{N_S} \sim \frac{N_{f0}}{N_S A} \tag{5.1}$$

Figure 14. (Continued)

where N_{f0}/N_S is the number of fires per time step that burn a single tree. It must be emphasized that this is a noncumulative distribution with N_f/N_S the number of fires per time step that burn A trees, $A = 1, 2, 3, 4, \ldots, G$ where G is the number of sites on the square grid.

The frequency–area distribution of model forest fires can be directly related to the frequency–area distribution of model tree clusters. A tree cluster is defined to be trees that will burn if a spark is dropped on any one of them and the cluster area A is the number of trees that will burn. If N is the number of tree clusters with area A and G is the total size of the system, we can write

$$\frac{N_f}{N_S} = \frac{NA}{G} f \tag{5.2}$$

where N_S is the total number of time steps that the model has been run, N_f/N_S is the probability that a fire of size A will occur at each time step, NA/G is the probability that a randomly dropped match will land on a cluster of size A, and f the sparking frequency. Combining (5.1) and (5.2) with $f \ll 1$ we have

$$N = \frac{N_0}{A^2} \tag{5.3}$$

with

$$N_0 = \frac{G N_{f0}}{f N_S} \tag{5.4}$$

where N_0 is the number of clusters on the grid containing only single trees. The number of fires N_f of area A is proportional to A^{-1} from (5.1), whereas the number of clusters N of area A is proportional to A^{-2} from (5.3). The cumulative number of clusters with areas greater than A, N_c, is given by

$$N_c = N_0 \int_A^\infty \frac{\mathrm{d}A}{A^2} = \frac{N_0}{A}. \tag{5.5}$$

The cumulative number of clusters with area greater than A has the same dependence on A as the noncumulative number of fires of size A given in (5.1).

A very simple inverse-cascade model can be introduced as an approximation to the forest-fire model. This process is referred to as being 'inverse' since the cascade proceeds from the smallest to the largest scales. Small clusters of trees coalesce to form larger clusters until the cluster is destroyed in a fire. It is assumed that clusters contain $2^0, 2^1, 2^2, \ldots, 2^n$ trees; the number of clusters with 2^n trees is N_n. Here, N_0 is the number of clusters consisting of one tree, as before. A set of population equations can be written to describe the behaviour of the inverse cascade

$$\frac{\mathrm{d}N_0}{\mathrm{d}t} = C_0 - C_{0,1} N_0^2 - D_0 N_0$$

$$\frac{\mathrm{d}N_1}{\mathrm{d}t} = \tfrac{1}{2} C_{0,1} N_0^2 - C_{1,2} N_1^2 - D_1 N_1$$

$$\frac{\mathrm{d}N_2}{\mathrm{d}t} = \tfrac{1}{2} C_{1,2} N_1^2 - C_{2,3} N_2^2 - D_2 N_2 \tag{5.6}$$

$$\vdots$$

$$\frac{\mathrm{d}N_n}{\mathrm{d}t} = \tfrac{1}{2} C_{n-1,n} N_{n-1}^2 - C_{n,n+1} N_n^2 - D_n N_n.$$

Trees are introduced only at the lowest $n = 0$ level. Two clusters of size 2^{n-1} coalesce to form a cluster of size 2^n. Particles cascade from small clusters to larger clusters. Fires destroy clusters of all sizes. The constant C_0 is the rate at which single particles are introduced to the cascade. The transition probability $C_{0,1}$ is the rate at which single particles combine to form particle pairs, $n = 1$. In this simple model, clusters of size 2^n are obtained only from the combination of two clusters of size 2^{n-1}; the rate at which this occurs is $\tfrac{1}{2}[C_{n-1,n} N_{n-1}^2]$. This is equivalent to a collision probability for clusters; since each cluster can combine with the N_{n-1} other clusters, the probability is proportional to N_{n-1}^2. Similarly, clusters of size 2^n are lost as they combine to form clusters of size 2^{n+1}; the rate at which this occurs is $C_{n,n+1} N_n^2$. Clusters of size 2^n are also lost directly at a rate $D_n N_n$. These are the fires in the forest-fire model and they are proportional to the number of clusters of size 2^n.

In terms of the forest-fire model, a unit of time t is the planting interval and C_0 is the rate at which single trees are planted. In the forest-fire model the number of trees in a cluster
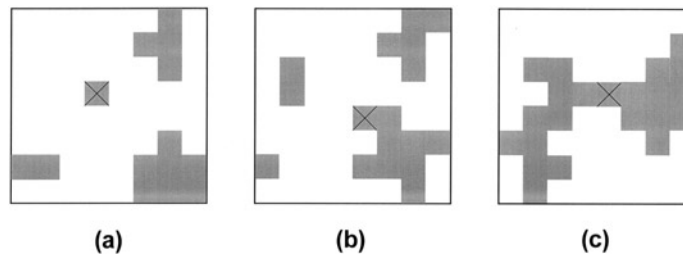
Figure 15. The trees marked by x have been added. (*a*) A new single-tree cluster is formed. (*b*) A pre-existing cluster has been increased in size by one. (*c*) The gap between two pre-existing clusters has been bridged so that the two clusters have coalesced to form a single cluster.

can take any integer value. The cascade model is a renormalization group approximation in the sense that clusters are boxed into sizes 2^n. It is similar to other dynamic renormalization group models that have been proposed (Newman and Wasserman 1990, Newman and Turcotte 1990, Newman and Knopoff 1990). In a sense it is also a mean-field approximation because a range of cluster sizes are treated as having the same mean size. An important assumption in the model is that cluster growth is dominated by the coalescence of clusters of approximately equal size. In the forest-fire model clusters increase in two ways as illustrated in figure 15. If a tree lands in a space adjacent to a cluster it increases in size by one. But if a tree bridges a gap between two clusters with n_1 and n_2 trees, a cluster with $n_1 + n_2 + 1$ trees is formed. In the analogy between the inverse-cascade model and the forest-fire model it is argued that the latter process dominates and is proportional to the number of clusters squared multiplied by the transition probability $C_{n,n+1}$. It is hypothesized that the addition of single trees to clusters is negligible compared with the coalescence of clusters. Although clusters of all sizes coalesce with each other, it is further hypothesized that the coalescence of clusters of approximately equal size (in the same renormalization bin) dominates. It is further assumed that the transition probability is proportional to the cluster area so that

$$C_{n,n+1} = 2^n \alpha C_0 \tag{5.7}$$

where α is a positive constant.

The dependence of the transition probability on area is similar to a collision cross section. An example would be the use of the set of equations (5.6) to model coagulation in a colloidal suspension. However, in our case the clusters are only in relative motion due to their growth. Statistically, the coalescence of randomly growing clusters is no different that the coalescence of clusters in random relative motion. The assumption that the transition probability is proportional to the cluster area is somewhat arbitrary and will be discussed further when solutions are given. In terms of the forest-fire analogy, the loss term $D_n N_n$ represents fires. The probability that a spark will hit a cluster is proportional to the cluster area so that we take

$$D_n = 2^n \beta C_0 \tag{5.8}$$

where β is a positive constant. The rate at which clusters of area 2^n are lost is proportional to the product of the area and the number of clusters; this is true for the forest-fire model. The constants α and β can be related to parameters in the forest-fire model.

The constant C_0 can be absorbed into the definition of time with no loss of generality

$$\tau = C_0 t. \tag{5.9}$$
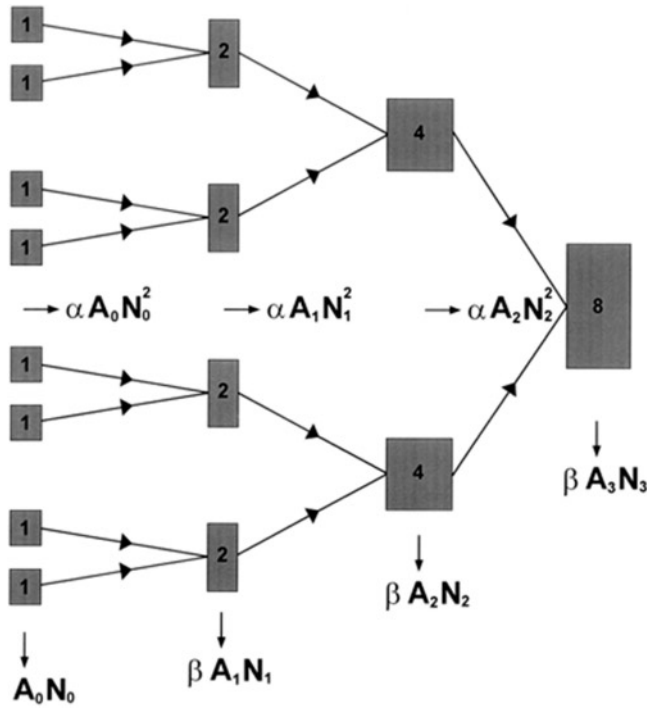
Figure 16. Schematic flow diagram for the inverse-cascade model. Clusters of size 2^0 combine to form clusters of size 2^1 with probability $\alpha A_0 N_0^2$ (where $A_0 = 2^0$) and clusters of size 2^0 are lost in fires with a probability $\beta A_0 N_0$. Similarly, clusters of size 2^1 combine to form clusters of size 2^2 with probability $\alpha A_1 N_0^2$ (where $A_1 = 2^1$) and clusters of size 2^1 are lost in fires with a probability $\beta A_1 N_0$.

Substitution of (5.7) to (5.9) into (5.6) gives

$$\frac{dN_0}{d\tau} = 1 - \alpha N_0^2 - \beta N_0$$

$$\frac{dN_1}{d\tau} = \tfrac{1}{2}\alpha N_0^2 - 2\alpha N_1^2 - 2\beta N_1$$

$$\frac{dN_2}{d\tau} = \tfrac{1}{2}2\alpha N_1^2 - 4\alpha N_2^2 - 4\beta N_2 \qquad (5.10)$$

$$\vdots$$

$$\frac{dN_n}{d\tau} = \tfrac{1}{2}2^{n-1}\alpha N_{n-1}^2 - 2^n\alpha N_n^2 - 2^n\beta N_n.$$

The behaviour of this inverse-cascade model is illustrated schematically in figure 16. The steady-state solution to this set of equations is obtained by setting $dN_n/d\tau = 0$ with the result

$$N_0 = \frac{-\beta + (\beta^2 + 4\alpha)^{1/2}}{2\alpha}$$

$$N_1 = \frac{-\beta + (\beta^2 + \alpha^2 N_0^2)^{1/2}}{2\alpha}$$

$$N_2 = \frac{-\beta + (\beta^2 + \alpha^2 N_1^2)^{1/2}}{2\alpha} \qquad (5.11)$$

$$\vdots$$

$$N_n = \frac{-\beta + (\beta^2 + \alpha^2 N_{n-1}^2)^{1/2}}{2\alpha}.$$

The second solutions of the quadratic equations can be discarded because they give negative values for N_n. The set of equations (5.11) generates an inverse cascade with a power-law frequency–area distribution if $\beta \ll \alpha$. In this limit it is found that

$$N_0 \approx \alpha^{-1/2}, \quad N_1 \approx \tfrac{1}{2}N_0, \quad N_2 \approx \tfrac{1}{2}N_1, \quad \ldots, \quad N_n \approx \tfrac{1}{2}N_{n-1}. \tag{5.12}$$

With $\alpha = N_0^{-2}$ and $A_n = 2^n$ this result gives

$$N_n = \frac{N_0}{2^n} = \frac{N_0}{A_n}. \tag{5.13}$$

This dependence is a direct consequence of the assumption that the transition probability $C_{n,n+1}$ has a linear dependence on cluster area in (5.7). This model has been extended to include the coalescence of clusters of all sizes (Gabrielov *et al* 1999); the inverse cascade remains scale invariant and (5.13) remains valid.

The binning used in this inverse-cascade model is equivalent to a logarithmic binning: that is, N_0 includes clusters of size 1, N_1 includes clusters of size 2 and 3, N_2 includes clusters of size 4–7, N_3 includes clusters of size 8–15, and so forth. When binned logarithmically, the noncumulative frequency–area power-law distribution yields the same power-law exponent as the cumulative distribution. When binned linearly, i.e. 1–2, 2–3, 3–4, ..., the power-law exponent for the noncumulative distribution is exactly 1.0 different from that of the corresponding cumulative distribution. Thus the result in (5.13) ($N_n = N_0/A_n$) is identical to the result applicable for the forest-fire model given in (5.5) ($N_c = N_0/A$). The simple inverse cascade reproduces the frequency–size distribution that is a characteristic of models that are said to exhibit self-organized critical behaviour.

This behaviour of the model is relatively easy to explain. As long as $\beta \ll 2^{-n}\alpha$, the loss of clusters of size 2^n and smaller due to fires is negligibly small compared with the number of clusters moving through the cascade. Significant numbers of clusters are lost only in the largest fires that terminate the cascade. Clusters of size 1 are continuously introduced and combine to form clusters of size 2, the clusters of size 2 combine to form clusters of size 4, and so forth. As long as a negligibly small number of clusters are lost in fires, the inverse cascade from small to large clusters results in the power-law relation (5.13). When $\beta \approx 2^{-n}\alpha$, large numbers of cluster are lost in fires and the inverse cascade is terminated.

In order to complete the analogy between the inverse-cascade model and the forest-fire model it is necessary to relate the loss parameter β to the sparking frequency f. The rate at which clusters are lost per time step in the inverse-cascade model is $2^n N_n \beta$, the rate at which clusters are lost per time step in the forest-fire model is $2^n N_n f/G$, equating these gives

$$\beta = \frac{f}{G}. \tag{5.14}$$

Substitution of this result and $\alpha \approx N_0^{-2}$ from equation (5.12) into equation (5.11) gives

$$
\begin{aligned}
\frac{N_1}{G} &= -\frac{f}{2}\left(\frac{N_0}{C}\right)^2 + \frac{1}{2}\left[f^2\left(\frac{N_0}{G}\right)^4 + \left(\frac{N_0}{G}\right)^2\right]^{1/2} \\
\frac{N_2}{G} &= -\frac{f}{2}\left(\frac{N_0}{C}\right)^2 + \frac{1}{2}\left[f^2\left(\frac{N_0}{G}\right)^4 + \left(\frac{N_1}{G}\right)^2\right]^{1/2} \\
&\vdots \\
\frac{N_n}{G} &= -\frac{f}{2}\left(\frac{N_0}{C}\right)^2 + \frac{1}{2}\left[f^2\left(\frac{N_0}{G}\right)^4 + \left(\frac{N_{n-1}}{G}\right)^2\right]^{1/2}.
\end{aligned}
\tag{5.15}
$$
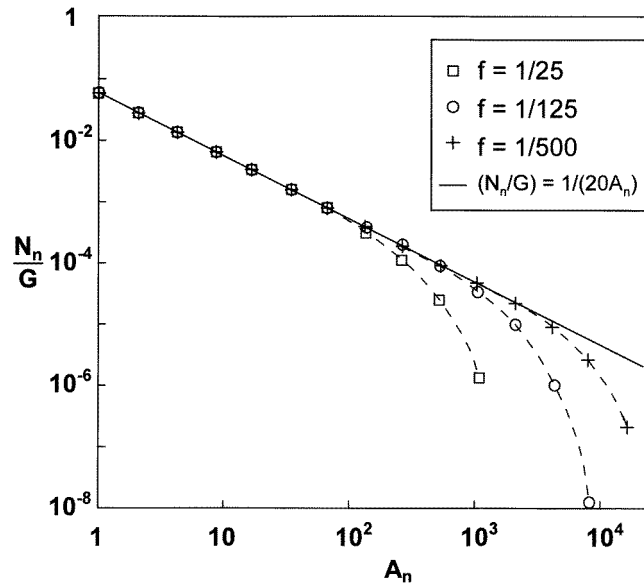
Figure 17. Theoretical frequency–area distributions for clusters obtained from the inverse-cascade model set of equations (5.15) with $N_0/G = 0.05$ and $1/f = 25$, 125, and 500. For each firing frequency, f, the number of clusters, N_n, of size $A_n = 2^n$, divided by the number of grid points G, is given as a function of A_n.

In the application of the inverse cascade approximation to the forest-fire model this result gives the complete cluster size distribution N_n/G when N_0/G and f are specified.

Taking $1/f = 125$, we see from figure 12 that $N_{f0}/N_S = 4 \times 10^{-4}$ and from (5.4) that $N_0/G = 0.05$. Using these two values for f and N_0/G, we calculate the resulting N_n/G for $n = 0, 1, 2, \ldots, 13$ using (5.15), and in figure 17 plot these with respect to the corresponding $A_n = 2^n$. Also included in figure 17 are results for $1/f = 25$ and $1/f = 500$, again using $N_0/G = 0.05$. The solid straight line in figure 18 represents the equation $(N_n/G = 0.05/A_n)$, a result of the limiting case equation $(N_n = N_0/A_n)$ (5.13) with the given $N_0/G = 0.05$. These results for the inverse-cascade model can be directly compared with the cluster statistics of the forest-fire model. The frequency–area distributions for clusters from forest-fire model runs with $G = 128^2 = 16\,384$ and $1/f = 25, 125, 500$ are given in figure 18. Clusters have been logarithmically binned in sizes $A_n = 2^n$. Comparing figures 17 and 18 it is seen that the agreement is excellent.

This inverse-cascade model can also be used to study the influence of a finite-size grid. For a finite-size grid the last term in the cascade from (5.10) is

$$\frac{\mathrm{d}N_n}{\mathrm{d}\tau} = \tfrac{1}{2}2^{n-1}\alpha N_{n-1}^2 - 2^n \beta N_n \tag{5.16}$$

where the size of the grid $G = 2^n$. In writing (5.16) we have considered a cluster that is equal in size to the grid. No further coalescence of clusters is possible and the cascade is terminated. Because clusters of size N_n cannot combine to form larger clusters, there is no $-2^n \beta N_n^2$ term in (5.16). Clusters of size N_n can only be lost in fires, resulting in the $-2^n \beta N_n$ term in (5.16)).

Substitution of (5.14) and $\alpha \approx N_0^{-2}$ into (5.16), with $\mathrm{d}N_n/\mathrm{d}\tau = 0$ gives

$$\frac{N_n}{G} = \frac{1}{4f}\left(\frac{G}{N_0}\right)^2 \left(\frac{N_{n-1}}{G}\right)^2. \tag{5.17}$$
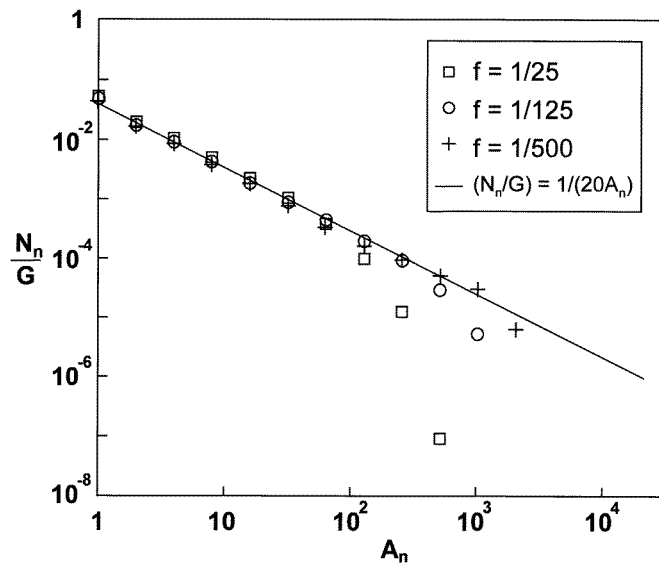
Figure 18. Frequency–area distributions of clusters in the forest-fire model with $G = 128^2$ and $1/f = 25, 125, 500$. The logarithmically binned number of clusters per grid point, N_n divided by G, of size $A_n = 2^n$, is given as a function of A_n. The theoretical results from the cascade model (figure 17) closely match the forest-fire model results presented in this figure.
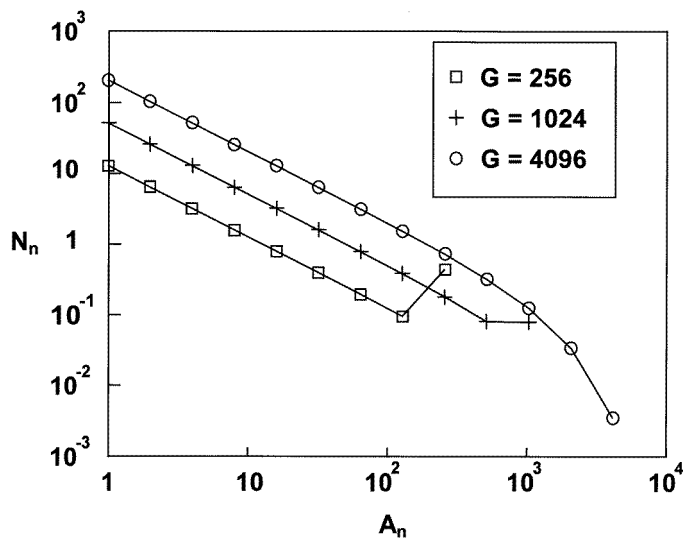
Figure 19. Frequency–area distributions of clusters with finite size grids with $G = 256, 1024, 4096$ from the inverse-cascade model, (5.15) and (5.17), $1/f = 125$ and $N_0/G = 0.05$. The number of clusters, N_n, of size $A_n = 2^n$, is given as a function of A_n.

Equation (5.17) is used only for the terminal step, $N_n = G$. For lower values of n, (5.15) is used. Taking $1/f = 125$, $N_0/G = 0.05$, and $G = 256, 1024$, and 4096 the resulting distributions of cluster sizes are given in figure 19. For the smaller grid sizes the peak in the number of largest clusters due to the termination of the cascade is clearly illustrated.

Although this inverse-cascade model is very simple, it appears to reproduce the basic behaviour of the forest-fire model and, therefore, the other cellular-automata models that are said to exhibit self-organized criticality. The behaviour of the model is easily explained. Particles are continuously introduced at the lowest-level clusters containing single particles. These clusters combine to form larger clusters and particles continuously migrate from smaller to larger clusters. This is the inverse cascade. This cascade is self-similar and thus leads to a power-law frequency–size distribution of clusters. Particles must also be lost. Although some particles are lost from all clusters, significant numbers of particles are lost only from the very largest clusters. This loss of particles leads to a break in the power-law behaviour and the termination of the cascade.

The inverse-cascade model can be applied to the sandpile and slider-block models in much the same way that it is applied to the forest-fire model. An initiation of an avalanche is equivalent to a spark being dropped on a cluster of trees. Tree clusters are equivalent to the metastable regions over which an avalanche will spread after rupture is initiated,

5.2. The forest-fire model versus the site-percolation model

It is instructive to compare the forest-fire model with the site-percolation model, which is known to exhibit critical behaviour. The site-percolation model also consists of a square grid of sites and can be discussed in terms of forest fires (Stauffer and Aharony 1992). In its standard formulation the site-percolation problem is specified in terms of the probability that there is a tree on a site p. If N_t is the number of trees on the grid of size G, then we have $p = N_t/G$. The probability p is increased until there is a cluster of trees that spans the grid, this is the critical probability p_c. If the forest-fire model is run without any fires it becomes the site-percolation model. This is a transient problem in which $p(t) = N(t)/G$ is a monotonically increasing function of time. We have $p = p_c$ when a cluster of trees first spans the grid. Monte Carlo simulations show that $p_c = 0.592\,75$ (Stinchcombe and Watson 1976).

It is recognized that the site-percolation model is a critical-point problem. The percolation probability, p, is a tuning parameter and the critical point corresponds to the critical percolation probability p_c. Many power-law scalings have been found to be valid in the vicinity of this critical point, i.e. $|p - p_c| \ll 1$. One of these power-law scalings is the frequency–area distribution of all clusters. The number of clusters N with size A scales with A according to

$$N \sim A^{-k} \tag{5.18}$$

where k is known as the Fisher exponent and takes a value $k = \frac{187}{91} = 2.055$ for a variety of two-dimensional percolation models (Stauffer and Aharony 1992). However, unlike the forest-fire model, the power-law frequency–area distribution of clusters is only valid when $N_t \approx p_c G$.

In order to compare the behaviour of the site-percolation model with the forest-fire model we consider a specific example of the transient behaviour of the forest-fire model without any fires. Trees are planted on randomly chosen grid sites until the entire grid is filled with trees. The time evolution of the number of clusters of various sizes is given in figure 20. Clusters are logarithmically binned in sizes $A_n = 2^n$ as described in the previous section. The number of clusters of size A_n, N_n, is given as a function of time t. The unit of time, $\Delta t = 1$, represents G (the total number of sites in the grid) attempts to plant trees. Initially, single-tree clusters, $A_0 = 2^0$, dominate; subsequently clusters grow and coalesce to form larger clusters of size 2^1, 2^2, 2^3, and so forth. The example given has $G = 1024^2$. This is a transient inverse cascade from smaller to larger clusters.

The frequency–area distributions of the binned clusters from figure 20 are given in figure 21
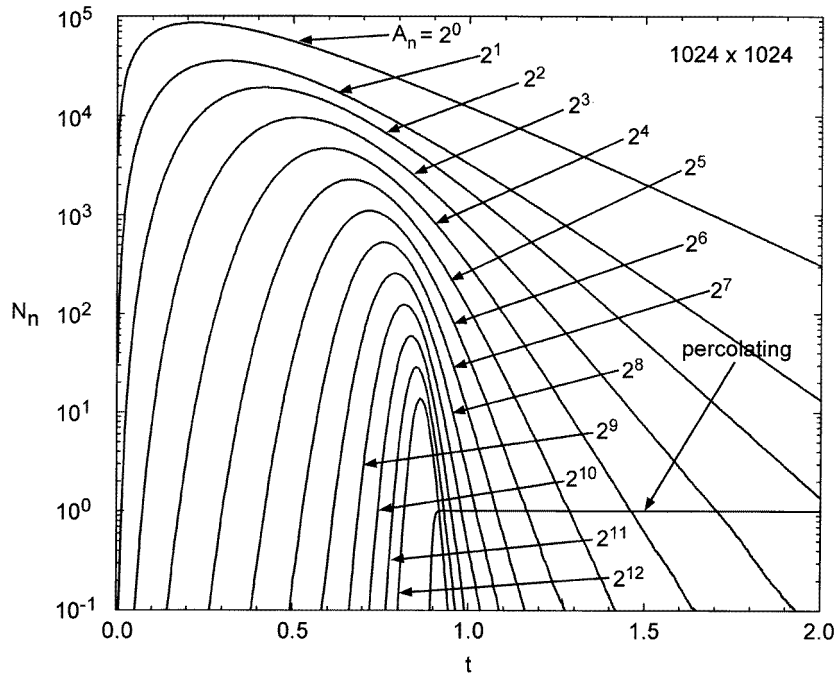
Figure 20. Dependence of the number of cluster, N_n, of a specified size A_n on time t for the forest-fire model without any fires. Results are given for logarithmically binned clusters with N_n being the number of clusters with area $A_n = 2^n$. For this example $G = 1024^2$. One unit of time, $\Delta t = 1.00$, is equivalent to G (the number of sites in the grid) time steps or attempts to plant trees. For instance, $t = 2.00$ represents the time after $2.097\,152 \times 10^6$ time steps, where an attempt is made at each time step to plant one tree.

for various times, t, and percolation probability, $p = N_t/G$. The total number of trees on the grid N_t is given as a function of time by the simple relation

$$p = \frac{N_t}{G} = [1 - \exp(-t)]. \tag{5.19}$$

The critical density associated with the percolation, $p_c = N_t/G = 0.592\,75$, is reached when $t = 0.898$. It is seen from figure 21 that the frequency–area distribution of clusters when $t = 0.898$ has a good power-law (fractal) distribution with an exponent of -0.96. In comparing this result with the Fisher exponent it is important to note that this is a logarithmically binned distribution, which is equivalent to a cumulative distribution. The equivalent noncumulative distribution when binned linearly will have an exponent exactly 1.0 lower, resulting in an exponent of -1.96, close to the expected Fisher exponent of -2.055.

Although this transient problem clearly exhibits an inverse-cascade behaviour, the resulting frequency–size distribution is only power-law at the critical percolation threshold. At other times, when the density of trees is either less than or greater than the critical values of $0.592\,75$, the distribution deviates strongly from a power law as illustrated in figure 21.

To further illustrate the difference between critical and self-organized critical behaviour we give an example of cluster size statistics for the forest-fire model. Again, the clusters are logarithmically binned in sizes $A_n = 2^n$. With $G = 128^2$ and $1/f = 700$ the number of binned cluster are given as a function of time in figure 22. The times at which large fires of various sizes occur are also given. It is seen that large fires occur when clusters of size 1 and
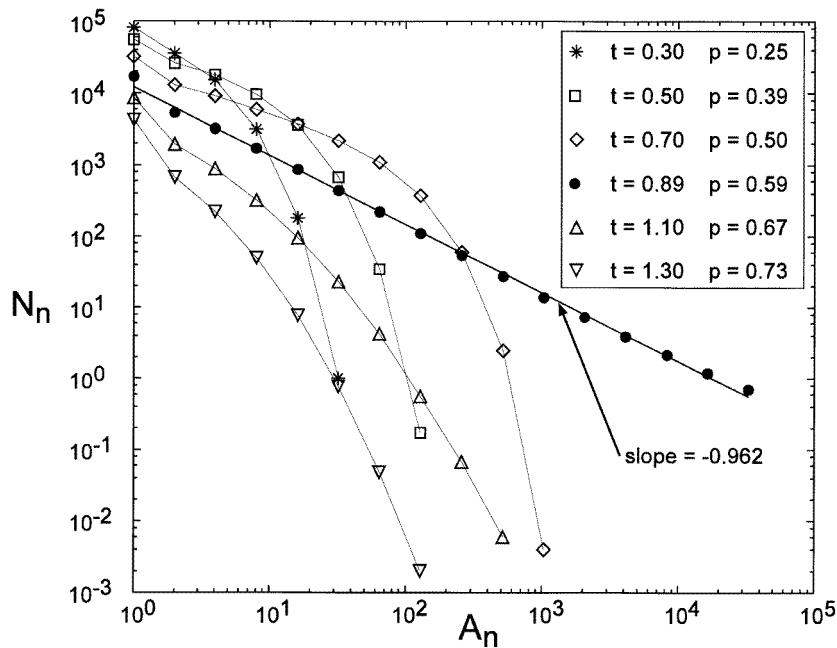
Figure 21. Frequency–area distributions of clusters for the transient behaviour of the forest-fire model without any fires. The logarithmically binned number of clusters, N_n, of size $A_n = 2^n$ is given as a function of A_n at various times, t, and corresponding percolation densities, p.

2 are at a minimum. The growth and fall in numbers of small clusters is very similar to that illustrated in figure 20. It is easily explained in terms of the density of trees. After a large fire the density is low and there is a transient filling of empty sites. As the sites fill the number of small clusters decrease until another major fire occurs. Although it is not possible to predict when large fires occur, it is seen that large fires do not occur when the numbers of small clusters is increasing.

A comparison of figures 21 and 22 clearly illustrate the differences between self-organized criticality and criticality. For the forest-fire model the numbers of binned clusters fluctuate but are well approximated by a power-law distribution at all times. The cascade of trees from small clusters to large clusters is continuous and can be approximated by the inverse-cascade model. The power-law (fractal) distribution of cluster sizes (and thus fire sizes) is a direct consequence of this continuous cascade.

The forest-fire model without fires is identical to the site-percolation model. This is a transient problem with the density of trees increasing with time until the grid is covered by trees. Power-law frequency–area distributions of tree clusters are only found near the critical value of the density of trees. This corresponds to the first cluster that spans the grid. The forest-fire model is a quasi-steady-state model. Trees are continuously planted and continuously destroyed in model fires. The cascade of trees from small to large cluster results in power-law frequency–size distribution for the clusters. A number of authors have discussed the relationship of self-organized criticality to criticality (Drossel *et al* 1994b, Sornette 1994, Paczuski 1995, Sornette *et al* 1995, Alencar *et al* 1997).
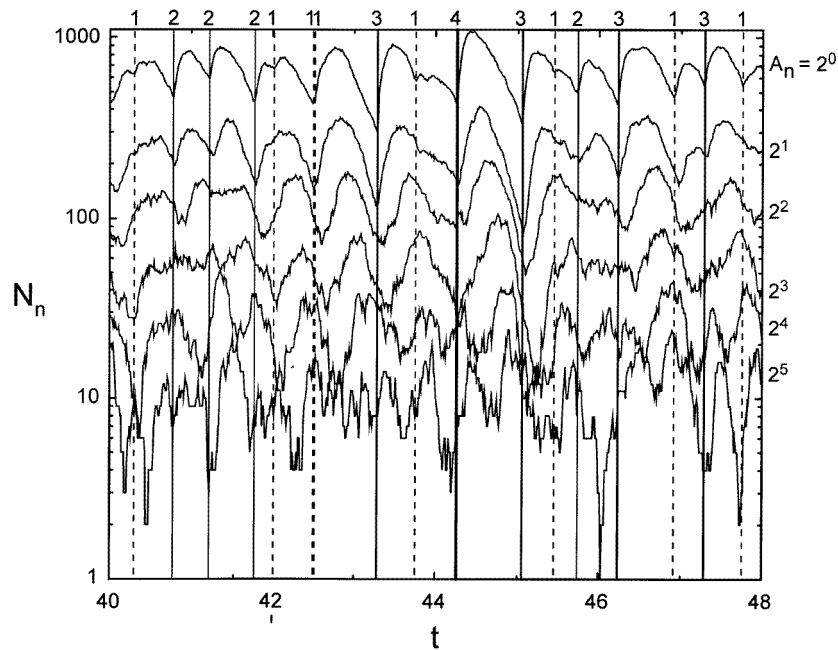
Figure 22. Dependence of the number of clusters, N_n, of a specified size A_n on time, t, for the forest-fire model. Results are given for logarithmically binned clusters, with N_n being the number of clusters with area $A_n = 2^n$. For this example $G = 128^2$ and $1/f = 700$. The unit of time, $\Delta t = 1.0$, corresponds to G (the number of sites on the grid) time steps, with an attempt to plant a tree at each time step. The vertical straight lines are instances during the model run at which large forest fires occur, where the numbers 1–4 represent, respectively, fires that have a size of between 10–20%, 20–30%, 30–40% and 40–50% of the size of the grid, G.

6. Other applications in the physical sciences

A wide variety of other applications of self-organized criticality in the physical sciences have been proposed. Grieger (1992) has considered applications to climate fluctuations, Nagel and Raschke (1992) have considered cloud formation, and Andrade *et al* (1998) have considered rainfall. Kawasaki and Okuzono (1996) have considered foams. Applications to solar flares have been given by Lu and Hamilton (1991) and Lu *et al* (1993) and to accretionary discs by Dendy *et al* (1998). Applications to plasma physics have been given by Carreras *et al* (1996), Kishimoto *et al* (1996), Medvedev *et al* (1996), Sivron (1998), and Rhodes *et al* (1999). Field *et al* (1995), Zieve *et al* (1996), Olson *et al* (1997), Bassler and Paczuski (1998), and Prozorov and Giller (1999) have considered vortex avalanches in super-conductors. Babcock and Westervelt (1990) and Che and Suhl (1990) have considered magnetic domain patterns. The Barkhausen effect and self-organized criticality have been studied by Cote and Meisel (1991) and by O'Brien and Weissman (1994). Cottrell (1996) has studied Andrade creep and Marchesoni and Patriarca (1994) dislocation networks. Corral *et al* (1995) and Mousseau (1996) have studied lattice models of integrate and fire oscillators. Pia and Nori (1991) have studied pinned lattices, Ciliberto and Laroche (1994) friction, and Sneppen and Jensen (1993) interface dynamics. Petri *et al* (1994) have considered microfracturing, Caldarelli *et al* (1996a) annealed disorders, Jogi and Sornette (1998) random directed polymers, Bernardes and Moreira (1995) fracture of fibrous materials, and Drossel and Schwabl (1995) autocatalytic surface reactions. Traffic flows and jams have been studied by Nagel and Herrmann (1993), Nagel and

Paczuski (1995) and Nagatani (1995, 1996). Applications have been made to the avalanches associated with interface depinning (Paczuski *et al* 1996, Jost 1998).

Some authors consider that the evolution of landforms is an example of self-organized criticality (Takayasu and Inaoka 1992, Rinaldo *et al* 1993, 1998, Rodriguez-Iturbe and Rinaldo 1997). A cellular-automata model for the development of river networks similar to the sandpile model was given by Chase (1992). The development of a fractal branching network is an essential feature of landform evolution. Because landform evolution is not associated with any form of 'avalanches', it seems to be inappropriate to associate landform evolution with self-organized criticality (Sapozhnikov and Foufoula-Georgiou 1996). This problem appears to be more closely associated with diffusion-limited aggregation (Masek and Turcotte 1993).

7. Applications in the biological sciences

7.1. The Game of Life

Models that exhibit self-organized criticality have also been applied to problems in the biological sciences. The first of these was the *Game of Life*, originally conceived by John Conway (Gardner 1970). This is a cellular-automata model that may approximate interactions between living organisms. A square grid of lattice points is considered. Each point represents an organism that is in one of two states: alive or dead. The fate of an organism depends on its eight nearest neighbours. The organism will die if there are less than two live neighbours (overexposure) and will also die with four or more alive neighbours (overcrowding). Otherwise, the organism will remain alive. At a dead site, a new organism will be born only if there are three live neighbours.

This model can be run from random initial conditions using a 'checkerboard' algorithm. The distribution will evolve until a stable critical population is reached. This stable state is then perturbed by selecting a random grid point and killing the organism if it is alive or introducing a live organism if the site is dead. An avalanche of births and deaths follow a perturbation. The frequency–area distribution of avalanches is a power law and satisfies (1.1) with $\alpha \approx 1.4$. A number of articles discuss in detail the relationship of the *Game of Life* to self-organized criticality, including Bak *et al* (1989), Bak (1992), Garcia *et al* (1993), Sales (1993), Alstrom and Leao (1994), Nordfalk and Alstrom (1996), Blok and Bergersen (1997), Newman *et al* (1997) and Ninagawa *et al* (1998).

7.2. The Bak–Sneppen model

Bak and Sneppen (1993) introduced a cellular-automata model for evolution. A one-dimensional linear set of L sites is considered and each site is assigned a random number f between 0 and 1. At each time step, the site with the smallest value of f is chosen. That site and the two neighbouring sites are then assigned new random values of f from the uniform distribution. A quasi-stationary state is established. In this state all sites have values, f, above a critical value, f_c. The sites have a uniform distribution of values in the range $f_c < f < 1$. The value of f_c is found to be 0.6670. At the next time step a new random number of f is assigned to the site with the smallest value of f. If the new value of f is less than f_c an avalanche is initiated until all sites again have values greater than f_c. Only adjacent sites participate in the avalanche. The number of sites that have values less than the critical value f_c define the size of an avalanche. If a site has smaller values several times, these are counted. As in other examples of self-organized criticality, the noncumulative frequency–size distribution of avalanches is power law with a slope very near unity; (1.1) is satisfied with $\alpha \approx 1.0$ for the

one-dimension model and $\alpha \approx 1.26$ for the two-dimensional model.

Considerable work has been carried out on a mean-field approach to this model (Flyvbjerg *et al* 1993, de Boer *et al* 1994, 1995, Ray and Jan 1994) and renormalization group methods have been used (Marsili 1994). A variety of other studies have been published (Plotnick and McKinney 1993, Maslov *et al* 1994, Paczuski *et al* 1994, 1996, Sutherland and Jacobs 1994, Adami 1995, Bak and Paczuski 1995a, b, Fernandez *et al* 1995, 1998, Ito 1995, Newman and Roberts 1995, Schmoltzi and Schuster 1995, Sneppen *et al* 1995, Boettcher and Paczuski 1996, 1997, Daerden and Vanderzande 1996, Sole and Bascompte 1996, Sole and Manrubia 1996, Sornette and Dornic 1996, Bak and Boettcher 1997, Boettcher 1997, Corral *et al* 1997, De Los Rios *et al* 1997, 1998, Fernandez and Plastino 1997, Pang 1997, Head and Rodgers 1998, Labzowsky and Pis'mak 1998, Tamarit *et al* 1998, Valleriani and Vega 1999).

In associating this model with evolution, the random numbers represent the fitness of the species (Kauffman and Levin 1987). The selection of the smallest random number represents the hypothesis of evolution that the least fit species is replaced or mutates. The influence of this mutation on the rest of the ecology is simulated by changing the fitness of neighbouring species on the lattice. An avalanche of mutations is considered to be the analogue of extinctions in the biological record. These avalanches are basically cascades of species with bad genes that become extinct. Sole *et al* (1999) have given a general discussion of criticality and scaling in terms of evolutionary ecology.

7.3. Applications to extinctions

The temporal variability associated with self-organized criticality is certainly consistent with the concept of punctuated evolution (Gould and Eldredge 1993). The fossil record provides ample evidence that evolution is associated with periods of rapid evolution of species and sudden rapid extinctions.

The largest of all extinctions was the Permo–Triassic extinction at 248 Ma (millions of years ago), which is estimated to have wiped out 96% of all marine species (Erwin 1993). While not the largest extinction, the Cretaceous–Tertiary extinction at 65 Ma has received the most attention. This can be attributed in part with its association with the extinction of the dinosaur. This extinction has been directly associated with a giant meteorite impact. This association was first documented by a discovery of a global iridium anomaly deposited at this time (Alvarez *et al* 1980). Subsequently other supporting features were found including impact glasses and tsunami deposits. This 10 km diameter impact is now associated with the Chicxulub impact crater in the northern Yucatan Peninsula, Mexico. Although there is little doubt that this impact occurred, there is still considerable controversy regarding its association with the extinction. A massive volcanic eruption of flood basalts in the Deccan Traps, India also occurred at about this time and has been associated with the extinction (Officer and Page 1996). Also, due to details of the timing, many paleontologists question the association of either the impact or the volcanism with the extinction. Other major extinctions occurred in the Late Devonian at 365 Ma with about a 75% loss of species, in the late Ordovician at 445 Ma with about 50% loss, and late Triassic at 220 Ma again with about a 50% loss. These are known as the 'big five' extinction events. It should also be noted that there is no evidence for a giant impact as a cause of the Permo–Triassic extinction (Retallack *et al* 1998).

It must be emphasized that the causes of major extinctions remains extremely controversial. This is summarized by the title of the book by Raup (1991): *Extinction: Bad Genes or Bad Luck?* Impacts and volcanic eruptions fall in the bad luck category. Climate changes have also been proposed as a cause of global extinctions (Sole *et al* 1996). The approach to extinctions discussed above, yielding self-organized criticality, certainly falls in the bad genes category.
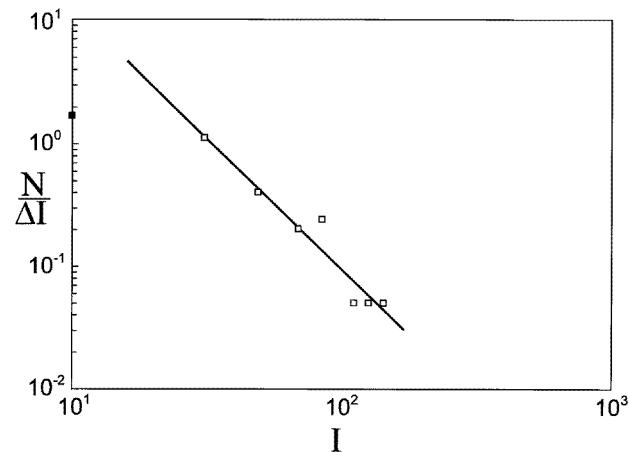
Figure 23. Noncumulative frequency–intensity statistics for extinctions in the geological record (Raup 1986). The measure of extinction intensity I is the number of extinctions of marine animal families during a geologic stage (time interval) during the Phanerozoic. The noncumulative (linearly binned) number of extinctions $N/\Delta I$ is given as a function of intensity I. The correlation with the power-law relation (7.1) is obtained taking $\alpha = 2.2$ and is given by the solid straight line.

It is clearly desirable to test whether this hypothesis is valid. One approach is to consider the frequency–size distribution of extinctions. Raup (1986) has given the intensities of 39 extinctions in the geological record. His noncumulative frequency-intensity distribution is given in figure 23. His measure of extinction is defined as the number of extinctions of marine animal families during a geological stage (time interval). The noncumulative (linearly binned) number of extinctions $N/\Delta I$ is given as a function of intensity I. This data is compared with the power-law relation:

$$\frac{N}{\Delta I} = \frac{C}{I^{\alpha}} \tag{7.1}$$

with $\alpha = 2.2$. Considering the limited nature and scatter of the data, the fit is reasonable. Although caution must be exercised, the results given in figure 22 tend to support extinctions as an example of self-organized criticality. Further support for this conclusion comes from power-law correlations of planktic foraminiferal extinctions (Patterson and Fowler 1996) and extinctions of Hawaiian avifauna (Keitt and Marquet 1996). Alternative models for extinctions have been given by Caldarelli *et al* (1998), Drossel (1998) and Killingback and Doebeli (1998). Newman and Sneppen (1996) introduced a coherent external noise model for avalanche behaviour and this model has been applied to extinctions (Newman 1996, 1997a, b, Sneppen and Newman 1997, Wilke and Martinetz 1997, Wilke *et al* 1998, Standish 1999). Hewzulla *et al* (1997) have discussed the application of self-organized criticality to extinctions in terms of time series.

7.4. Other studies

A variety of other studies have been carried out relating self-organized criticality to biological problems. O'Toole *et al* (1999) have considered termite nest architecture. Vandewalle and Ausloos (1995) have considered applications to phylogenetic (evolutionary) trees. Herz and Hopfield (1995) and da Silva *et al* (1998) have related slider-block models to the neural reverberations of spiking nerve cells. Chialvo and Bak (1999) have considered learning and

memory. And Barabasi *et al* (1996) have considered applications to breathing avalanches in the lung.

8. Applications in the social sciences

Applications of self-organized criticality to the social sciences are much more controversial than applications in the physical and biological sciences. Certainly the social sciences involve complex interactions, but it is unclear whether these interactions can be qualified beyond applying random statistics such as Gaussian distributions and Brownian motions. The most quantitative of the social sciences is economics and power-law (fractal) distributions are often found (Mandelbrot 1982, Levy *et al* 1996).

Stock markets are characterized by crashes, which certainly resemble avalanches (Scheinkman and Woodford 1994, Mantegna and Stanley 1997). Bak *et al* (1993, 1997) have considered whether the behaviour of stock markets is an example of self-organized criticality, but relatively little other work has been done. It has been argued that there are log-periodic (complex fractal) fluctuations prior to stock market crashes (Feigenbaum and Freund 1996, Sornette *et al* 1996, Sornette and Johansen 1997), but both their validity and interpretation remain uncertain.

One interesting application of self-organized criticality is to wars (Roberts and Turcotte 1998). It is first shown that the statistical distribution of war intensities is well approximated by a power-law distribution. This distribution is then interpreted in terms of the forest-fire model. An obvious measure of the intensity of a war I is the number of battle deaths. The frequency–size distribution of war intensities is then simply the dependence of the number of wars, N, on the number of battle deaths, I. Richardson (1941) was the first to carry out this type of study using logarithmic binning. He considered 82 wars between 1820 and 1929 and found that $N = 1$ war had $\log I = 7.0 \pm 0.5$ (i.e. between 3 160 000 and 31 600 000 battle deaths, $N = 3$ wars with $\log I = 6.0 \pm 0.5$ (i.e. between 316 000 and 3 160 000 battle deaths), $N = 16$ wars with $\log I = 5.0 \pm 0.5$ (i.e. between 31 600 and 316 000 battle deaths), and $N = 62$ wars with $\log I = 4.0 \pm 0.5$ (i.e. between 3 160 and 31 600 battle deaths). Richardson (1941) pointed out that his statistical data correlated well with the relation

$$N = CI^{-D} \tag{8.1}$$

taking $D = 1.0$. Richardson (1960) extended and updated his studies in his book *Statistics of Deadly Quarrels*. Because logarithmic binning was used, Richardson's results were equivalent to cumulative distributions.

One of the major criticisms of the use of the number of battle deaths as a measure of a war's intensity is the substantial change in the global population over the period of time considered. A more logical measure would be the ratio of battle deaths to the world's population prior to the war. However, for the earlier wars, estimates of the world's population are unreliable. For this reason Levy (1983) defines the intensity of a war I as the ratio of battle deaths to the population of Europe in millions at the time of the war.

Levy (1983) has tabulated the intensities of 119 wars beginning with the war of the League of Venice in 1495–97 and ending with the Vietnam War in 1965–73. The largest wars were the Second World War with $I = 93\,665$ and the First World War with $I = 57\,616$. The cumulative number of wars, N_c, with intensity greater than I, has been converted into a noncumulative distribution using the derivative technique. The derivative dN_c/dI is obtained by taking the mean slope of a specified number of adjacent data points, in this case five. The dependence of dN_c/dI on I for the Levy (1983) distribution of war intensities is given in figure 24. If a fractal
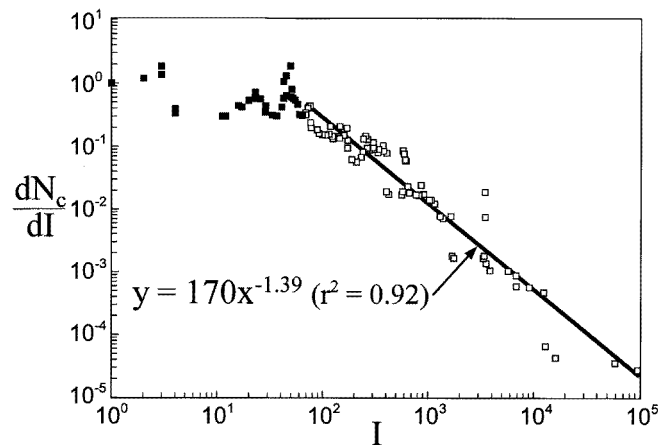
Figure 24. Noncumulative frequency–intensity distribution of wars based on the Levy (1983) tabulation of war intensities. The noncumulative number of wars, $-\mathrm{d}N_c/\mathrm{d}I$, is given as a function of I. The larger wars correlate well with the power-law relation (8.2) taking $D = 1.39$.

(power-law) distribution is applicable we would expect a good correlation with the relation

$$\frac{\mathrm{d}N_c}{\mathrm{d}I} = CI^{-D}. \tag{8.2}$$

This correlation is illustrated in figure 24 taking $D = 1.39$. This is the best-fit result for wars with intensities greater than 100. The fit is seen to be quite good for war intensities greater than about $I = 30$ and extends over about three orders of magnitude of data. The deviation for small wars may be real or may be due to the incompleteness of the data set.

Although it is certainly of interest that war intensities obey power-law (fractal) statistics, a more fundamental question is why? Are wars an example of a self-organized critical phenomena? In particular, can an association be made between the number of battle deaths in a war and the number of trees that burn (the area) in a forest fire? If this is done, the frequency–size distributions for wars given in figure 24 is remarkably similar to the frequency–size distributions for forest fires given in figure 14. For wars we have $\alpha = 1.39$ from (8.2). For the four data sets for forest fires given in figure 14 we have $\alpha = 1.3, 1.3, 1.4, 1.5$. We can explain this behaviour for forest fires in terms of the forest-fire model, a key question is whether this explanation is also valid for wars.

In terms of the forest-fire model a spark ignites a tree and the model fire consumes the entire cluster to which this tree belongs. This is similar to real forest fires where ignition of the forest must take place for a fire to take place and the fire then spreads through the contiguous flammable material.

Similarly, a war must began in a manner similar to the ignition of a forest. One country may invade another country, or a prominent politician may be assassinated. The war will then spread over the contiguous region of metastable countries. Such regions of metastability could be the countries of the Middle East (Iran, Iraq, Syria, Israel, Egypt, etc) or of the former Yugoslavia (Serbia, Bosnia, Croatia, etc). These are then the metastable clusters. In some cases the metastable clusters could combine. Albania and Greece bridge the gap between the metastable clusters of the Middle East and the former Yugoslavia.

Saperstein (1995) has discussed the relation of wars to complexity theory in a general way. One can qualitatively discuss the breakdown of order in the world in a similar manner to the 'forest fires' in the forest-fire model. In the forest-fire model, sometimes a match starts a

fire and sometimes it does not. Some fires are large and some are small. But the frequency–size distribution is power-law. In terms of world order there are small conflicts that may or may not grow into major wars. The stabilizing and destabilizing influences are clearly very complex. The results we have shown indicate that world order behaves as a self-organized critical system independent of the efforts made to control and stabilizer interactions between people and countries.

It is easy to argue that the results given here cannot be significant. The introduction of weapons of mass destruction, particularly the atom bomb, must change global interactions and the associated wars. However, as we have shown, the noncumulative frequency–area statistics of real forest fires are well approximated by power-law distributions with exponents near 1.3. Again it can be argued that attempts to extinguish fires, changing land use practices, and other human interventions should have affected the resulting distribution of fires. But a variety of correlations show that the power-law, frequency–area distributions of these complex phenomena remain valid.

9. Concluding remarks

A number of models and natural phenomena have been discussed that may or may not exhibit self-organized critical behaviour. It is desirable to provide a 'clean' definition of what self-organized criticality is, but there is not a universally accepted definition. In fact, some authors would submit that self-organized critical behaviour is the same as critical behaviour.

This inability to provide a generally accepted definition for self-organized criticality is quite similar to the concept of fractals. Mandelbrot (1982), in his book *The Fractal Geometry of Nature*, did not provide a definition of a fractal distribution. Certainly it is agreed that the Cantor set is a fractal. But what about a power-law distribution of fragment masses? Are all or only some of the power-laws observed in nature fractal? In some cases, two power-law distributions are found in nature for different parts of a parameter space, are these both fractal? Mathematicians tend to favour restricted definitions, engineers broad definitions, and physicists are somewhere in between. Although the definition of a fractal remains elusive, the concept is widely used and has great utility. What about self-organized criticality?

Most authors would agree that the original sandpile model proposed by Bak *et al* (1987) is an example of self-organized critical behaviour. But, this agreement does not extend to the slider-block and forest-fire models. It is certainly possible to provide a rigorous mathematically-based definition of self-organized criticality. For example, full self-similarity would be required. However, such a restricted definition may not address the real utility of the basic concept. The essential question is whether a broad range of real complex phenomena exhibits similar behaviour under very broad conditions. This seems to be true for earthquakes, landslides and forest fires. It may also be true for a variety of other examples in the physical, biological and social sciences. A few examples are species extinctions, epidemics, stock-market crashes and wars.

A universal feature of these phenomena is that they are driven systems that involve 'avalanches' with a fractal (power-law) frequency–size distribution. There is a steady-state 'input' and the 'output' occurs in the 'avalanches'. Although it has not been widely established, there is evidence that a system with self-organized criticality is on the 'edge' of chaos. Adjacent solutions exhibit power-law divergence in time, whereas chaotic solutions exhibit exponential divergence (a positive Lyapunov exponent).

The simple forest-fire model exhibits many of the characteristics associated with self-organized criticality. This forest-fire model is also closely related to the site-percolation model that exhibits critical behaviour. The transient forest-fire model without fires is identical to

the site-percolation model, the critical point is when a cluster has formed that crosses the grid. For both the quasi-steady-state forest-fire model with fires, and the transient forest-fire model without fires, there is an inverse cascade of trees from small to large clusters. In the quasi-steady-state forest-fire model this cascade gives a power-law frequency–area distribution for both the smaller clusters of trees and the forest fires. In the transient cascade associated with the site-percolation problem, a power-law distribution is found only at a critical density of trees. The quasi steady-state, self-similar cascade can explain major differences between critical and self-organized critical behaviour, at least for some models.

The above discussion has focused on the power-law (fractal) distributions of the 'avalanches'. However, there are other important aspects of the behaviour of models and natural phenomena that are associated with self-organized criticality. One of these concerns correlation lengths. Studies of critical phenomena emphasize the systematic increase in the correlation length as the critical point is approached. It has not been established whether there are systematic temporal variations in correlation lengths in models with self-organized criticality. There is observational evidence for a well-defined correlation length for seismic activation prior to a major earthquake.

As indicated by the large number of references given in this paper, there is a broad interest in self-organized critical behaviour, both in terms of understanding its behaviour and in terms of applications. What has been written above is certainly only a progress report on a rapidly evolving subject, with concepts and applications of self-organizing criticality being published at a rapid rate.

References

ACT Bush Fire Council 1996 Electronic Data *Firebreak Web Site* (msowww.anu.edu.au/˜ barling/firebreak/firehistory.html)
Adami C 1995 *Phys. Lett.* A **203** 29–32
Aki K 1981 *Earthquake Prediction* ed D Simpson and P Richards (Washington, DC: American Geophysical Union) pp 566–74
——1987 *J. Geophys. Res.* **92** 1349–1355
Albano E V 1994 *J. Phys. A: Math. Gen.* **27** L881–6
——1995 *Physica* A **216** 213–226
Alencar A M, Andrade J S and Lucena L S 1997 *Phys. Rev.* E **56** R2379–82
Ali A A and Dhar D 1995a *Phys. Rev.* E **51** R2705–8
——1995b *Phys. Rev.* E **52** 4804–16
Alstrom P 1988 *Phys. Rev.* A **38** 4905–6
Alstrom P and Leao J 1994 *Phys. Rev.* E **49** R2507–8
Alvarez L W, Alvarez W, Asaro F and Michael H V 1980 *Science* **208** 1095–108
Andrade R F S, Schellnhuber H J and Claussen M 1998 *Physica* A **254** 557–68
Babcock K L and Westervelt R M 1990 *Phys. Rev. Lett.* **64** 2168–71
Bak P 1990 *Physica* A **163** 403–9
——1992 *Physica* A **191** 41–6
——1996 *How Nature Works: The Science of Self-Organized Criticality* (New York: Copernicus) p 212
Bak P and Boettcher S 1997 *Physica* D **107** 143–50
Bak P and Chen K 1995 *Fractals in the Earth Sciences* ed C Barton and P La Pointe (New York: Plenum) pp 227–36
Bak P, Chen K and Creutz M 1989 *Nature* **342** 780–2

Bak P, Chen K, Scheinkman J and Woodford M 1993 *Ric. Econ.* **47** 3–30
Bak P, Chen K and Tang C 1992 *Phys. Lett.* A **147** 297–300
Bak P, Christensen K and Olami Z 1994 *Am. Geophys. Un. Geophys. Mono.* **83** 69–74
Bak P and Creutz M 1994 *Fractals in Science* ed A Bunde and S Havlin (Berlin: Springer) pp 27–47
Bak P and Paczuski M 1995a *Proc. Natl Acad. Sci. USA* **92** 6689–96
——1995b *Fractals* **3** 415–29
Bak P, Paczuski M and Shubik M 1997 *Physica* A **246** 430–53
Bak P and Sneppen K 1993 *Phys. Rev. Lett.* **71** 4083–6
Bak P and Tang C 1989 *J. Geophys. Res.* **94** 15 635–7
Bak P, Tang C and Wiesenfeld K 1987 *Phys. Rev. Lett.* **59** 381–4
——1988 *Phys. Rev.* A **38** 364–74
Barabasi A L, Buldyrev S V, Stanley H E and Suki B 1996 *Phys. Rev. Lett.* **76** 2192–5
Barriere B and Turcotte D L 1991 *Geophys. Res. Lett.* **18** 2011–14
——1994 *Phys. Rev.* E **49** 1151–60
Bassler K E and Paczuski M 1998 *Phys. Rev. Lett.* **81** 3761–4
Baumann G and Wolf D E 1996 *Phys. Rev.* E **54** 4504–7
Ben-Hur A and Biham O 1996 *Phys. Rev.* E **53** R1317–20
Bernardes A T and Moreira J G 1995 *J. Physique* I **5** 1135–41
Bhowal A 1997 *Physica* A **247** 327–30
Blok H J and Bergersen B 1997 *Phys. Rev.* E **55** 6249–52
Blodgett T A 1998 Erosion rates on the NE escarpment of the Eastern Cordillera, Bolivia, derived from aerial
    photographs and thematic mapper images *PhD Thesis* Cornell University, p 139
Boettcher S 1997 *Phys. Rev.* E **56** 6466–74
Boettcher S and Paczuski M 1996 *Phys. Rev. Lett.* **76** 348–51
——1997 *Phys. Rev. Lett.* **79** 889–92
Boguna M and Corral A 1997 *Phys. Rev. Lett.* **78** 4950–3
Bonabeau E and Lederer P 1994 *J. Phys. A: Math. Gen.* **27** L243–50
Bowman D D, Ouillon G, Sammis C G, Sornette A and Sornette D 1998 *J. Geophys. Res.* **103** 24 359–72
Bretz M, Cunningham J B, Kurczynski P L and Nori F 1992 *Phys. Rev. Lett.* **69** 2431–4
Broker H M 1996 *Europhys. Lett.* **36** 321–4
Broker H M and Grassberger P 1997 *Phys. Rev.* E **56** R4918–21
Brown S R Scholz C H and Rundle J B 1991 *Geophys. Res. Lett.* **18** 215–18
Buchholtz V and Poschel T 1996 *J. Stat. Phys.* **84** 1373–6
Bufe C G and Varnes D J 1993 *J. Geophys. Res.* **98** 9871–83
Burridge R and Knopoff L 1967 *Seis. Soc. Am. Bull.* **57** 341–71
Cafiero R, Loreto V, Pietronero L, Vespignani A and Zapperi S 1995 *Europhys. Lett.* **29** 111–16
Caldarelli G, Di Tolla F D and Petri G A 1996a *Phys. Rev. Lett.* **77** 2503–6
Caldarelli G, Higgs P G and McKane A J 1998 *J. Theor. Biol.* **193** 345–58
Caldarelli G, Maritan A and Vendruscolo M 1996b *Europhys. Lett.* **35** 481–5
Carlson J M 1991a *J. Geophys. Res.* **96** 4255–67
——1991b *Phys. Rev.* A **44** 6226–32
Carlson J M, Chayes J T, Grannan E R and Swindle G H 1990 *Phys. Rev.* A **42** 2467–70
Carlson J M, Grannan E R, Singh C and Swindle G H 1993a *Phys. Rev.* E **48** 688–98
Carlson J M, Grannan E R and Swindle G H 1993b *Phys. Rev.* E **47** 93–105
Carlson J M and Langer J S 1989a *Phys. Rev. Lett.* **62** 2632–5
——1989b *Phys. Rev.* A **40** 6470–84
Carlson J M, Langer J S and Shaw B E 1994 *Rev. Mod. Phys.* **66** 657–70
Carlson J M, Langer J S, Shaw B E and Tang C 1991 *Phys. Rev.* A **44** 884–97
Carlson J M and Swindle G H 1995 *Proc. Natl Acad. Sci. USA* **92** 6712–19
Carreras B A, Newman D, Lynch V E and Diamond P H 1996 *Phys. Plasmas* **3** 2903–11
Cartwright J H E, Hernandez-Garcia E and Piro O 1997 *Phys. Rev. Lett.* **79** 527–30
Ceva H 1995 *Phys. Rev.* E **52** 154–8
Ceva H and Luzuriaga J 1998 *Phys. Lett.* A **250** 275–80
Chabanol M L and Hakim V 1997 *Phys. Rev.* E **56** R2343–6
Chang D, Lee S C and Tzeng W J 1995 *Phys. Rev.* E **51** 5515–19
Chase C G 1992 *Geomorphology* **5** 39–57
Che X and Suhl H 1990 *Phys. Rev. Lett.* **64** 1670–3
Chen K, Bak P and Obukhov S P 1991 *Phys. Rev.* A **43** 625–30

Chessa A, Marinari E and Vespignani A 1998 *Phys. Rev. Lett.* **80** 4217–20
Chessa A, Stanley H E, Vespignani A and Zapperi S 1999 *Phys. Rev.* E **59** R12–15
Chhabra A B, Feigenbaum M J, Kadanoff L P, Kolan A J and Procaccia I 1993 *Phys. Rev.* E **47** 3099–123
Chialvo D R and Bak P 1999 *Neuroscience* **90** 1137–48
Christensen K, Corral A, Frette V, Feder J and Jossang T 1996 *Phys. Rev. Lett.* **77** 107–10
Christensen K, Flyvbjerg H and Olami Z 1993 *Phys. Rev. Lett.* **71** 2737–40
Christensen K, Fogedby H C and Jensen H J 1991 *J. Stat. Phys.* **63** 653–84
Christensen K and Olami Z 1992a *J. Geophys. Res.* **97** 8729–35
——1992b *Phys. Rev.* A **46** 1829–38
——1993 *Phys. Rev.* E **48** 3361–72
Christensen K, Olami Z and Bak P 1992 *Phys. Rev. Lett.* **68** 2417–20
Ciliberto S and Laroche C 1994 *J. Physique* I **4** 223–35
Clar S, Drossel B, Schenk K and Schwabl F 1999 *Physica* A **266** 153–9
Clar S, Drossel B and Schwabl F 1994 *Phys. Rev.* E **50** 1009–18
——1995 *Phys. Rev. Lett.* **75** 2722–5
——1996 *J. Phys.: Condens. Matter* **8** 6803–24
Clar S, Schenk K and Schwabl F 1997 *Phys. Rev.* E **55** 2174–83
Cohen S 1977 *J. Geophys. Res.* **82** 3781–96
Corral A, Perez C J, Diaz-Guilera A and Arenas A 1995 *Phys. Rev. Lett.* **74** 118–21
——1997 *Phys. Rev. Lett.* **78** 1492–5
Cote P J and Meisel L V 1991 *Phys. Rev. Lett.* **67** 1334–7
Cottrell A H 1996 *Phil. Mag.* A **74** 1041–6
Cowie P A, Vanneste C and Sornette D 1993 *J. Geophys. Res.* **98** 21 809–21
Crisanti A, Jensen M H, Vulpiani A and Paladin G 1992 *Phys. Rev.* A **46** R7363–6
Daerden F and Vanderzande C 1996 *Phys. Rev.* E **53** 4723–8
——1998 *Physica* A **256** 533–46
da Silva L, Papa A R R and de Souza A M C 1998 *Phys. Lett.* A **242** 343–8
de Boer J, Derrida B, Flyvbjerg H, Jackson A D and Wettig T 1994 *Phys. Rev. Lett.* **73** 906–9
de Boer J, Jackson A D and Wettig T 1995 *Phys. Rev.* E **51** 1059–74
De Los Rios P, Valleriani A and Vega J L 1997 *Phys. Rev.* E **56** 4876–9
——1998 *Phys. Rev.* E **57** 6451–9
Dendy R O, Helander P and Tagger M 1998 *Astron. Astrophys.* **337** 962–5
Densmore A L, Anderson R S, McAdoo B G and Ellis M A 1997 *Science* **275** 369–72
de Sousa Vieira M 1992 *Phys. Rev.* A **46** 6288–93
——1995 *Phys. Lett.* A **198** 407–14
——1996 *Phys. Rev.* E **54** 5925–8
de Sousa Vieira M and Lichtenberg A J 1996 *Phys. Rev.* E **53** 1441–5
de Sousa Vieira M, Vasconcelos G L and Nagel S R 1993 *Phys. Rev.* E **47** R2221–4
Dhar D 1990 *Phys. Rev. Lett.* **64** 1613–16
——1992 *Physica* A **186** 82–7
——1996 *Physica* A **224** 162–8
——1999 *Physica* A **263** 4–25
Dhar D and Majumdar S N 1990 *J. Phys. A: Math. Gen.* **23** 4333–50
Dhar D and Manna S S 1994 *Phys. Rev.* E **49** 2684–7
Dhar D and Ramaswamy R 1989 *Phys. Rev. Lett.* **63** 1659–62
Dhar D, Ruelle P, Sen S and Verma D N 1995 *J. Phys. A: Math. Gen.* **28** 805–31
Diaz-Guilera A 1992 *Phys. Rev.* A **45** 8551–8
Dickman R, Vespignani A and Zapperi S 1998 *Phys. Rev.* E **57** 5095–105
Dietrich J H 1972 *J. Geophys. Res.* **77** 3771–81
Ding E J and Lu Y N 1993 *Phys. Rev. Lett.* **70** 3627–30
Drossel B 1996 *Phys. Rev. Lett.* **76** 936–9
——1997 *Physica* A **236** 309–20
——1998 *Phys. Rev. Lett.* **81** 5011–14
Drossel B, Clar S and Schwabl F 1993 *Phys. Rev. Lett.* **71** 3739–42
——1994a *Z. Naturforsch.* A **49** 846–50
——1994b *Phys. Rev.* E **50** 2399–402
Drossel B and Schwabl F 1992a *Phys. Rev. Lett.* **69** 1629–32
——1992b *Physica* A **191** 47–50

——1993a *Fractals* **1** 1022–9
——1993b *Physica* A **199** 183–97
——1994 *Physica* A **204** 212–29
——1995 *Appl. Phys.* **60** 597–600
Edney S D, Robinson P A and Chisholm D 1998 *Phys. Rev.* E **58** 5395–402
Erwin D H 1993 *The Great Paleozoic Crisis: Life and Death in the Permian* (New York: Columbia University Press)
    p 327
Espanol P 1994 *Phys. Rev.* E **50** 227–35
Evernden J F 1970 *Seis. Soc. Am. Bull.* **60** 393–446
Evesque P 1991a *Europhys. Lett.* **14** 427–32
——1991b *Phys. Rev.* A **43** 2720–40
Evesque P, Fargeix D, Habib P, Luong M P and Porion P 1993 *Phys. Rev.* E **47** 2326–32
Evesque P and Rajchenbach J 1989 *Phys. Rev. Lett.* **62** 44–6
Family F 1994 *Fractals in the Natural and Applied Sciences* ed M M Novak (Amsterdam: Elsevier) pp 109–17
Feder J 1995 *Fractals* **3** 431–43
Feder H J S and Feder J 1991 *Phys. Rev. Lett.* **66** 2669–72
Feigenbaum J A and Freund P G O 1996 *Int. J. Mod. Phys.* B **10** 3737–45
Ferguson C D, Klein W and Rundle J B 1998 *Comput. Phys.* **12** 34–40
Fernandez J and Plastino A 1997 *Phys. Rev.* E **56** 841–7
Fernandez J, Plastino A and Diambra L 1995 *Phys. Rev.* E **52** 5700–3
Fernandez J, Plastino A, Diambra L and Mostaccio C 1998 *Phys. Rev.* E **57** 5897–903
Field S, Witt J, Nori F and Ling X 1995 *Phys. Rev. Lett.* **74** 1206–9
Fisher D S, Dahmen K, Ramanatham S and Ben-Zion Y 1997 *Phys. Rev. Lett.* **78** 4885–8
Flyvbjerg H 1996 *Phys. Rev. Lett.* **76** 940–3
Flyvbjerg H, Sneppen K and Bak P 1993 *Phys. Rev. Lett.* **71** 4087–90
Frette V 1993 *Phys. Rev. Lett.* **70** 2762–5
Frette V, Christensen K, Malthe-Sorenssen A, Feder J, Jossang T and Meakin P 1996 *Nature* **379** 49–52
Gabrielov A, Newman W I and Turcotte D L 1999 *Phys. Rev.* E at press
Garcia J B C, Gomes M A F, Juh T I, Ren T I and Sales T R M 1993 *Phys. Rev.* E **48** 3345–51
Garcia-Pelayo R 1994 *Phys. Rev.* E **49** 4903–6
Gardner M 1970 *Sci. Am.* **223** 120–3
Gaveau B and Schulman L S 1991 *J. Phys. A: Math. Gen.* **24** L475–80
Geller R J 1997 *Geophys. J. Int.* **131** 425–50
Geller R J, Jackson D D, Kagan Y Y and Mulargia F 1997 *Science* **275** 1616–17
Gil L and Sornette D 1996 *Phys. Rev. Lett.* **76** 3991–4
Gould S J and Eldredge N 1993 *Nature* **366** 223–7
Grassberger P 1993 *J. Phys. A: Math. Gen.* **26** 2081–9
——1994 *Phys. Rev.* E **49** 2436–43
Grassberger P and Kantz H 1991 *J. Stat. Phys.* **63** 685–700
Grassberger P and Manna S S 1990 *J. Physique* **51** 1077–98
Grieger B 1992 *Physica* A **191** 51–6
Grinstein G, Lee D H and Sachdev S 1990 *Phys. Rev. Lett.* **64** 1927–30
Grumbacher S K, McEwen K M, Halverson D A, Jacobs D T and Lindner J 1993 *Am. J. Phys.* **61** 329–35
Gutenberg B and Richter CF 1954 *Seismicity of the Earth and Associated Phenomenon* 2nd edn (Princeton, NJ:
    Princeton University Press) p 310
Hager W, Linz S J and Hanggi P 1997 *Europhys. Lett.* **40** 393–8
Hainzl S, Zöller G and Kurths J 1999 *J. Geophys. Res.* **104** 7243–53
Harp E L and Jibson R L 1995 *US Geol. Survey Open File Report* pp 95–213
Harvard Centroid-Moment Tensor Data Base 1997 (Cambridge: Harvard University)
Head D A and Rodgers G J 1997a *Phys. Rev.* E **55** 2573–9
——1997b *Phys. Rev.* E **56** 1976-80
——1998 *J. Phys. A: Math. Gen.* **31** 3977–88
——1999 *J. Phys. A: Math. Gen.* **32** 1387–93
Held G A, Solina D H, Keane D T, Haag W J, Horn P M and Grinstein G 1990 *Phys. Rev. Lett.* **65** 1120–3
Henley C L 1993 *Phys. Rev. Lett.* **71** 2741–4
Hergarten S and Neugebauer H J 1998 *Geophys. Res. Lett.* **25** 801–4
Herz A V M and Hopfield J J 1995 *Phys. Res. Lett.* **75** 1222–5
Hewzulla D, Boulter M C, Benton M J and Halley J M 1997 *Phil. Trans. R. Soc.* B **354** 463–9

Heyerdahl E, Swanson F, Berry D and Agee K 1994 *Fire History Database of the Western United States* Electronic
    data at H J Andrews LTER database (www.fsl.orst.edu/lter/datafr.htm)
Hiscott R N, Colella A, Pezard P, Lovell M A and Malinverno A 1992 *Proc. Ocean Drill. Program, Sci. Results* **126**
    75–96
Honecker A and Peschel I 1996 *Physica* A **229** 478–500
——1997 *Physica* A **239** 509–30
Hovius N, Stark C P and Allen P A 1997 *Geology* **25** 231–4
Huang J, Narkounskaia G and Turcotte D L 1992 *Geophys. J. Int.* **111** 259–69
Huang J and Turcotte D L 1990a *Geophys. Res. Lett.* **17** 223–6
——1990b *Nature* **348** 234–6
——1992 *Pure Appl. Geophys.* **138** 569–89
Huang Y, Saleur H, Sammis C and Sornette D 1998 *Europhys. Lett.* **41** 43–8
Ito K 1992 *Pure Appl. Geophys.* **138** 531–48
——1995 *Phys. Rev.* E **52** 3232–3
Ito K and Matsuzaki M 1990 *J. Geophys. Res.* **95** 6853–60
Ivashkevich E V 1996 *Phys. Rev. Lett.* **76** 3368–71
Ivashkevich E V, Ktitarev D V and Priezzhev V B 1994 *Physica* A **209** 347–60
Ivashkevich E V and Priezzhev V B 1998 *Physica* A **254** 97–116
Jaeger H M, Liu C H and Nagel S R 1989 *Phys. Rev. Lett.* **62** 40–3
Janowsky S A and Laberge C A 1993 *J. Phys. A: Math. Gen.* **26** L973–80
Jensen H J 1998 *Self-Organized Criticality: Emergent Complex Behaviour in Physical and Biological Sciences*
    (Cambridge: Cambridge University Press) p 153
Jensen H J, Christensen K and Fogedby H C 1989 *Phys. Rev.* B **40** 7425–7
Jogi P and Sornette D 1998 *Phys. Rev.* E **57** 6936–43
Johansen A 1994 *Physica* D **78** 186–93
Jost M 1998 *Phys. Rev.* E **57** 2634–9
Kadanoff L P, Nagel S R, Wu L and Zhou S M 1989 *Phys. Rev.* A **39** 6524–33
Kagan Y Y 1997 *Geophys. J. Int.* **131** 505–25
Kasischke E S and French N H F 1995 *Remote Sens. Environ.* **51** 263–75
Katori M and Kobayashi H 1993 *Physica* A **199** 461–77
Kauffman S A and Levin S 1987 *J. Theor. Biol.* **128** 11–45
Kawasaki K and Okuzono T 1996 *Fractals* **4** 339–48
Keilis-Borok V I 1996 *Proc. Natl Acad. Sci. USA* **93** 3748–55
Keitt T H and Marquet P A 1996 *J. Theor. Biol.* **182** 161–7
Kertesz J and Kiss L B 1990 *J. Phys. A: Math. Gen.* **23** L433–40
Killingback T and Doebeli M 1998 *J. Theor. Biol.* **191** 335–40
Kinouchi O, Pinho S T R and Prado C P C 1998 *Phys. Rev.* E **58** 3997–4000
Kinouchi O and Prado C P C 1999 *Phys. Rev.* E **59** 4964–9
Kishimoto Y, Tajima T, Horton W, LeBrun M J and Kim J Y 1996 *Phys. Plasmas* **3** 1289–307
Knopoff L, Landoni J A and Abinante M S 1993 *Phys. Rev.* A **46** 7445–9
Kutnjak-Urbanc B, Havlin S and Stanley H E 1996a *Phys. Rev.* E **54** 6109–13
Kutnjak-Urbanc B, Zapperi S, Milosevic S and Stanley H E 1996b *Phys. Rev.* E **54** 272–7
Labzowsky G L and Pis'mak Y M 1998 *Phys. Lett.* A **246** 377–83
Lauritsen K B, Zapperi S and Stanley H E 1996 *Phys. Rev.* E **54** 2483–8
Leary P C 1997 *Geophys. J. Int.* **131** 451–66
Leung K T, Andersen J V and Sornette D 1998a *Phys. Rev. Lett.* **80** 1916–19
——1998b *Physica* A **254** 85–96
Leung K T, Muller J and Andersen J V 1997 *J. Physique* I **7** 423–9
Levy J S 1983 *War in the Modern Great Power System 1495–1975* (Lexington, KY: University of Kentucky Press)
    p 215
Levy M, Solomon S and Ram G 1996 *Int. J. Mod. Phys.* C **7** 65–72
Lin B and Taylor P L 1994 *Phys. Rev.* E **49** 3940–7
Lise S and Jensen H J 1996 *Phys. Rev. Lett.* **76** 2326–9
Lise S and Stella A L 1998 *Phys. Rev.* E **57** 3633–6
Liu W S, Lu Y N and Ding E J 1995 *Phys. Rev.* E **51** 1916–28
Lorenz E N 1963 *J. Atmos. Sci.* **20** 130–41
Loreto V, Pietronero L, Vespignani A and Zapperi S 1995a *Phys. Rev. Lett.* **75** 465–8
——1995b *Fractals* **3** 445–52

Loreto V, Vespignani A and Zapperi S 1996 *J. Phys. A: Math. Gen.* **29** 2981–3004

Lu C, Takayasu H, Tretyakov A Y, Takayasu M and Yumoto S 1998 *Phys. Lett.* A **242** 349–54

Lu E T and Hamilton R J 1991 *Astrophys. J.* **380** L89–92

Lu E T, Hamilton R J, McTiernan J M and Bromund K R 1993 *Astrophys. J.* **412** 841–52

Lu Y N, Liu W S and Ding E J 1994 *Phys. Rev. Lett.* **72** 4005–8

Lubeck S 1997 *Phys. Rev.* E **56** 1590–4

——1998 *Phys. Rev.* E **58** 2957–64

Lubeck S, Tadic B and Usadel K D 1996 *Phys. Rev.* E **53** 2182–9

Lubeck S and Usadel K D 1997 *Phys. Rev.* E **55** 4095–9

Main I 1996 *Rev. Geophys.* **34** 433–62

Majumdar S S and Dhar D 1991 *J. Phys. A: Math. Gen.* **24** L357–62

——1992 *Physica* A **185** 129–45

Malamud B D, Morein G and Turcotte D L 1998 *Science* **281** 1840–2

Malamud B D and Turcotte D L 1999 *Natural Hazards* at press

Malthe-Sorenssen A 1996 *Phys. Rev.* E **54** 2261–5

Mandelbrot B B 1982 *The Fractal Geometry of Nature* (San Francisco, CA: Freeman) p 460

Manna S S 1990 *J. Stat. Phys.* **59** 509–21

——1991a *Physica* A **179** 249–68

——1991b *J. Phys. A: Math. Gen.* **24** L363–9

Manna S S and Giri D 1997 *Phys. Rev.* E **56** R4914–17

Manna S S and Khakhar D V 1998 *Phys. Rev.* E **58** R6935–8

Manna S S, Kiss L B and Kertesz J 1990 *J. Stat. Phys.* **61** 923–32

Mantegna R N and Stanley H E 1997 *The Physics of Complex Systems* ed F Mallamace and H E Stanley (Amsterdam: IOS) pp 473–89

Marchesoni F and Patriarca M 1994 *Phys. Rev. Lett.* **72** 4101–4

Marsili M 1994 *Europhys. Lett.* **28** 385–90

Masek J G and Turcotte D L 1993 *Earth Planet. Sci. Lett.* **119** 379–86

Maslov S, Paczuski M and Bak P 1994 *Phys. Rev. Lett.* **73** 2162–5

Maslov S and Zhang Y C 1995 *Phys. Rev. Lett.* **75** 1550–3

Matsuzaki M and Takayasu H 1991 *J. Geophys. Res.* **96** 19 925–31

May R M 1976 *Nature* **261** 459–67

McCloskey J 1993 *Geophys. J. Int.* **115** 538–51

McCloskey J and Bean C J 1992 *Geophys. Res. Lett.* **19** 119–22

——1994 *Science* **266** 410–12

McCloskey J, Bean C J and O'Reilly B 1993 *Geophys. Res. Lett.* **20** 1403–6

McNamara B and Wiesenfeld K 1990 *Phys. Rev.* A **41** 1867–73

Medvedev M V, Diamond P H and Carreras B A 1996 *Phys. Plasmas* **3** 3745–53

Mehta A and Barker G C 1994a *Europhys. Lett.* **27** 501–6

——1994b *Rep. Prog. Phys.* **57** 383–416

Middleton A A and Tang C 1995 *Phys. Rev. Lett.* **74** 742–5

Milshtein E, Biham O and Solomon S 1998 *Phys. Rev.* E **58** 303–10

Morein G and Turcotte D L 1998 *Phys. Rev.* E **57** 5126–34

Morein G, Turcotte D L and Gabrielov A 1997 *Geophys. J. Int.* **131** 552–8

Mossner W K, Drossel B and Schwabl F 1992 *Physica* A **190** 205–17

Mousseau N 1996 *Phys. Rev. Lett.* **77** 968–71

Nagatani T 1995 *J. Phys. A: Math. Gen.* **28** L119–24

——1996 *Fractals* **4** 279–83

Nagel K and Herrmann H J 1993 *Physica* A **199** 254–69

Nagel K and Paczuski M 1995 *Phys. Rev.* E **51** 2909–18

Nagel K and Raschke E 1992 *Physica* A **182** 519–31

Nagel S R 1992 *Rev. Mod. Phys.* **64** 321–5

Nakanishi H 1990 *Phys. Rev.* A **41** 7086–9

——1991 *Phys. Rev.* A **43** 6613–21

Narkounskaia G, Huang J and Turcotte D L 1992 *J. Stat. Phys.* **67** 1151–83

Narkounskaia G and Turcotte D L 1992 *Geophys. J. Int.* **111** 250–8

National Interagency Fire Center 1996 Electronic data from Andrea Olson, Fire Management Branch, US Fish and Wildlife Service, Boise, ID

Newman M E J 1996 *Proc. R. Soc.* B **263** 1605–10

——1997a *Physica* D **107** 293–6
——1997b *J. Theor. Biol.* **189** 235–52
Newman M E J, Fraser S M, Sneppen K and Tozier W A 1997 *Phys. Lett.* A **228** 202–4
Newman M E J and Roberts B W 1995 *Proc. R. Soc.* B **263** 1605–10
Newman M E J and Sneppen K 1996 *Phys. Rev.* E **54** 6226–31
Newman W I and Knopoff L 1990 *Int. J. Fract.* **43** 19–24
Newman W I and Turcotte D L 1990 *Geophys. J.* **100** 433–9
Newman W I and Wasserman I 1990 *Astrophys. J.* **354** 411–17
Nilsen T H, Bartow J A, Frizzell V A Jr and Sims J D 1975 *US Geology Survey Open File Report* pp 75–277
Ninagawa S, Yoneda M and Hirose S 1998 *Physica* D **118** 49–52
Noever D A 1993 *Phys. Rev.* E **47** 724–5
Nordfalk J and Alstrom P 1996 *Phys. Rev.* E **54** R1025–8
O-Brien K P and Weissman M B 1992 *Phys. Rev.* A **46** R4475–8
——1994 *Phys. Rev.* E **50** 3446–52
Officer C B and Page J 1996 *The Great Dinosaur Extinction Controversy* (New York: Addison-Wesley) p 209
Ohmori H and Hirano M 1988 *Z. Geomorph. NF Suppl.* **67** 55–65
Ohmori H and Sugai T 1995 *Z. Geomorph. NF Suppl.* **101** 149–64
Olami Z and Christensen K 1992 *Phys. Rev.* A **46** R1720–3
Olami Z, Feder H J S and Christensen K 1992 *Phys. Rev. Lett.* **68** 1244–7
Olson C J, Reichhardt C, Groth J, Field S B and Nori F 1997 *Physica* C **290** 89–97
O'Toole D V, Robinson P A and Myerscough 1999 *J. Theor. Biol.* **198** 305–27
Otsuka M 1972 *Phys. Earth Planet. Int.* **6** 311–15
Pacheco J, Scholz C H and Sykes L R 1992 *Nature* **355** 71–3
Paczuski M 1995 *Phys. Rev.* E **52** R2137–40
Paczuski M and Bak P 1993 *Phys. Rev.* E **48** R3214–16
Paczuski M and Boettcher S 1996 *Phys. Rev. Lett.* **77** 111–14
Paczuski M, Maslov S and Bak P 1994 *Europhys. Lett.* **27** 97–102
——1996 *Phys. Rev.* E **53** 414–43
Pang N N 1997 *Int. J. Mod. Phys.* B **11** 1411–44
Patterson R T and Fowler A D 1996 *Geology* **24** 215–18
Pelletier J D, Malamud B D, Blodgett T and Turcotte D L 1997 *Eng. Geol.* **48** 255–68
Pepke S L and Carlson J M 1994 *Phys. Rev.* E **50** 236–42
Pepke S L, Carlson J M and Shaw B E 1994 *J. Geophys. Res.* **99** 6769–88
Petri A, Paparo G, Vespignani A, Alippi A and Costantini M 1994 *Phys. Rev. Lett.* **73** 3423–6
Pia O and Nori F 1991 *Phys. Rev. Lett.* **67** 919–22
Pietronero L 1995 *Fractals* **3** 405–14
Pietronero L and Schneider W R 1991 *Phys. Rev. Lett.* **66** 2336–9
Pietronero L, Vespignani A and Zapperi S 1994 *Phys. Rev. Lett.* **72** 1690–3
Pinho S T R, Prado C P C and Salinas S R 1997 *Phys. Rev.* E **55** 2159–65
Plotnick R E and McKinney M L 1993 *Palaios* **8** 202–12
Plourde B, Nori F and Bretz M 1993 *Phys. Rev. Lett.* **71** 2749–52
Priezzhev V B 1994 *J. Stat. Phys.* **74** 955–79
Priezzhev V B, Ktitarev D V and Ivashkevich E V 1996 *Phys. Rev. Lett.* **76** 2093–6
Priezzhev V B and Sneppen K 1998 *Phys. Rev.* E **58** 6959–63
Prado C P C and Olami Z 1992 *Phys. Rev.* A **45** 665–9
Prozorov R and Giller D 1999 *Phys. Rev.* B **59** 14 687–91
Puhl H 1992 *Physica* A **182** 295–319
Raup D M 1986 *Science* **231** 1529–33
——1991 *Extinction: Bad Genes or Bad Luck?* (New York: Norton) p 210
Ray T S and Jan N 1994 *Phys. Rev. Lett.* **72** 4045–8
Retallack G J, Seyedolali A, Krull E S, Holser W T, Ambers C P and Kyte F T 1998 *Geology* **26** 979–82
Rhodes C J and Anderson R M 1996a *Nature* **381** 600–2
——1996b *Phil. Trans. R. Soc.* B **251** 1679–88
Rhodes C J, Jensen H J and Anderson R M 1997 *Proc. R. Soc.* B **264** 1639–46
Rhodes T L, Moyer R A, Groebner R, Doyle E J, Lehmer R, Peebles W A and Rettig C L 1999 *Phys. Lett.* A **253** 181–6
Richardson L F 1941 *Nature* **148** 598
Richardson L F 1960 *Statistics of Deadly Quarrels* (Pittsburgh, PA: Boxwood) p 373

Rinaldo A I, Rodriguez-Iturbe I and Rigon R 1998 *Ann. Rev. Earth Planet. Sci.* **26** 289–327

Rinaldo A I, Rodriguez-Iturbe I, Rigon R, Ijjasz-Vasquez E and Bras R L 1993 *Phys. Rev. Lett.* **70** 822–6

Roberts D C and Turcotte D L 1998 *Fractals* **6** 351–7

Robinson P A 1994 *Phys. Rev.* E **49** 3919–26

Rodriguez-Iturbe I and Rinaldo A 1997 *Fractal River Basins: Chance and Self-Organization* (Cambridge: Cambridge University Press) p 547

Rosendahl J, Vekic M and Kelley J 1993 *Phys. Rev.* E **47** 1401–4

Rosendahl J, Vekic M and Rutledge J E 1994 *Phys. Rev. Lett.* **73** 537–40

Rothman D H, Grotzinger J P and Flemings P 1994 *J. Sed. Petrol.* A **64** 59–67

Roux S and Guyon E 1989 *J. Phys. A: Math. Gen.* **22** 3693–705

Rundle J B 1993 *J. Geophys. Res.* **98** 21 943–9

Rundle J B and Brown S R 1991 *J. Stat. Phys.* **65** 403–12

Rundle J B, Gross S, Klein W, Ferguson C and Turcotte D L 1997 *Tectonophysics* **277** 147–64

Rundle J B and Jackson D D 1977 *Seis. Soc. Am. Bull.* **67** 1363–77

Rundle J B and Klein W 1989 *Phys. Rev. Lett.* **63** 171–4

——1993 *J. Stat. Phys.* **72** 405–12

——1995 *Nonlinear Proc. Geophys.* **2** 61–79

Rundle J B, Klein W and Gross S 1996a *Phys. Rev. Lett.* **76** 4285–8

——1996b *Reduction and Predictability of Natural Disasters* ed J B Rundle, D L Turcotte and W Klein (Reading, MA: Addison-Wesley) pp 167–203

Rundle J B, Klein W, Gross S and Turcotte D L 1995 *Phys. Rev. Lett.* **75** 1658–61

——1996c *Reduction and Predictability of Natural Disasters* ed J B Rundle, D L Turcotte and W Klein (Reading, MA: Addison-Wesley) pp 261–72

Ruskin H J and Feng Y 1997 *Physica* A **245** 453–60

Sales T R M 1993 *J. Phys. A: Math. Gen.* **26** 6187–93

Sammis C, King G and Biegel R 1987 *Pure Appl. Geophys.* **125** 777–812

Saperstein A M 1995 *Am. Sci.* **83** 548–57

Sapozhnikov V B and Foufoula-Georgiou E 1996 *Water Resour. Res.* **32** 1109–12

Sasaki Y, Abe M and Hirano I 1991 *J. Japan. Sci., Eng. Geol.* **32** 1–11

Scheinkman J A and Woodford M 1994 *Am. Econ. Rev.* **84** 417–21

Schmittbuhl J, Vilotte J P and Roux S 1993 *Europhys. Lett.* **21** 375–80

——1996 *J. Geophys. Res.* **101** 27 741–64

Scholz C H 1991 *Spontaneous Formation of Space Time Structure and Criticality* ed T Riste and D Sherrington (Amsterdam: Kluwer) pp 41–56

——1997 *Bull. Seism. Soc. Am.* **87** 1074–7

Schmoltzi K and Schuster H G 1995 *Phys. Rev.* E **52** 5273–80

SCSN (Southern California Seismographic Network) Catalog 1995 (Pasadena, CA: California Institute of Technology)

Senatorski P 1994 *Physica* D **76** 420–35

——1995 *J. Geophys. Res.* **100** 24 111–20

Shaw B E 1993a *Geophys. Res. Lett.* **20** 643–6

——1993b *Geophys. Res. Lett.* **20** 907–10

——1994 *Geophys. Res. Lett.* **21** 1983–6

——1995 *J. Geophys. Res.* **100** 18 239–51

——1997 *J. Geophys. Res.* **102** 27 367–77

Shaw B E, Carlson J M and Langer J S 1992 *J. Geophys. Res.* **97** 479–88

Sivron R 1998 *Astrophys. J.* **503** L57–61

Sneppen K, Bak P, Flyvbjerg H and Jensen M H 1995 *Proc. Natl Acad. Sci. USA* **92** 5209–13

Sneppen K and Jensen M H 1993 *Phys. Rev. Lett.* **71** 101–4

Sneppen K and Newman M E J 1997 *Physica* D **110** 209–22

Socolar J E S, Grinstein G and Jayaprakash C 1993 *Phys. Rev.* E **47** 2366–76

Sole R V and Bascompte J 1996 *Proc. R. Soc.* B **263** 161–8

Sole R V, Bascompte J and Manrubia S C 1996 *Proc. R. Soc.* B **263** 1407–13

Sole R V and Manrubia S C 1995a *Phys. Rev.* E **51** 6250–3

——1995b *J. Theor. Biol.* **173** 31–40

——1996 *Phys. Rev.* E **54** R42–5

Sole R V, Manrubia S C, Benton M, Kauffman S and Bak P 1999 *Trends Ecol. Evol.* **14** 156–60

Somfai E, Czirok A and Vicsek T 1994 *J. Phys. A: Math. Gen.* **27** L757–63

Sornette A and Sornette D 1989 *Europhys. Lett.* **9** 197–202

Sornette D 1992 *J. Physique* I **2** 2089–96
——1994 *J. Physique* I **4** 209–21
Sornette D, Davy P and Sornette A 1990 *J. Geophys. Res.* **95** 17 353–61
Sornette D and Dornic I 1996 *Phys. Rev.* E **54** 3334–8
Sornette D and Johansen A 1997 *Physica* A **245** 411–22
Sornette D, Johansen A and Bouchard J P 1996 *J. Physique* I **6** 167–75
Sornette D, Johansen A and Dornic I 1995 *J. Physique* I **5** 325–35
Speer E R 1993 *J. Stat. Phys.* **71** 61–74
Standish R K 1999 *Phys. Rev.* E **59** 1545–50
Stauffer D and Aharony A 1992 *Introduction to Percolation Theory* 2nd edn (London: Taylor and Francis) p 181
Stella A L, Tebaldi C and Caldarelli G 1995 *Phys. Rev.* E **52** 72–5
Stinchcombe R B and Watson B P 1976 *J. Phys. C: Solid State Phys.* **9** 3221–47
Strocka B, Duarte J A M S and Schreckenberg M 1995 *J. Physique* I **5** 1233–8
Sugai R, Ohmori H and Hirano M 1994 *Trans. Japan, Geomorph. Un.* **15** 233–51
Sutherland B R and Jacobs A E 1994 *Complex Systems* **8** 385–405
Tadic B and Dhar D 1997 *Phys. Rev. Lett.* **79** 1519–22
Tadic B, Nowak U, Usadel K D, Ramaswamy R and Padlewski S 1992 *Phys. Rev.* A **45** 8536–45
Takayasu H and Inaoka H 1992 *Phys. Rev. Lett.* **68** 966–9
Tamarit F A, Cannas S A and Tsallis C 1998 *Eur. Phys. J.* B **1** 545–8
Tang C and Bak P 1988a *J. Stat. Phys.* **51** 797–802
——1988b *Phys. Rev. Lett.* **60** 2347–50
Tsuchiya T and Katori M 1999 *J. Phys. A: Math. Gen.* **32** 1629–41
Turcotte D L 1997 *Fractals and Chaos in Geology and Geophysics* 2nd edn (Cambridge: Cambridge University Press)
    p 398
Turcotte D L 1999 *Phys. Earth Planet. Inter.* **111** 275–93
Turcotte D L, Malamud B D, Morein G and Newman W I 1999 *Physica* A **268** 629–43
Umbanhowar P B, Melo F and Swinney H L 1996 *Nature* **382** 793–6
Valleriani A and Vega J L 1999 *J. Phys. A: Math. Gen.* **32** 105–14
Vandewalle N and Ausloos M 1995 *J. Physique* I **5** 1011–25
Vasconcelos G L, de Sousa Vieira M and Nagel S R 1991 *Phys. Rev.* A **44** R7869–72
——1992 *Physica* A **191** 69–74
Vergeles M 1997 *Phys. Rev.* E **55** 6264–5
Vergeles M, Maritan A and Banavar J R 1997 *Phys. Rev.* E **55** 1998–2000
Vespignani A and Zapperi S 1997 *Phys. Rev. Lett.* **78** 4793–8
——1998 *Phys. Rev.* E **57** 6345–62
Vespignani A, Zapperi S and Pietronero L 1995 *Phys. Rev.* E **51** 1711–24
Whitehouse I E and Griffiths G A 1983 *Geology* **11** 331–4
Wiesenfeld K, Tang C and Bak P 1989 *J. Stat. Phys.* **54** 1441–58
Wiesenfeld K, Theiler J and McNamara B 1990 *Phys. Rev. Lett.* **65** 949–52
Wilke C, Altmeyer S and Martinetz T 1998 *Physica* D **120** 401–17
Wilke C and Martinetz T 1997 *Phys. Rev.* E **56** 7128–31
Xu H J and Knopoff L 1994 *Phys. Rev.* E **50** 3577–81
Yokoi Y, Carr J R and Watters R J 1995 *Env. Eng. Geosci.* **1** 75–81
Zapperi S, Lauritsen K B and Stanley H E 1995 *Phys. Rev. Lett.* **75** 4071–4
Zhang S D 1997 *Phys. Lett.* A **233** 317–22
Zhang S D, Huang Z P and Ding E J 1996 *J. Phys. A: Math. Gen.* **29** 4445–55
Zhang Y C 1989 *Phys. Rev. Lett.* **63** 470–3
Zieve R J, Rosenbaum T F, Jaeger H M, Seidler G T, Crabtree G W and Welp U 1996 *Phys. Rev.* B **53** 11 849–54